Available online at www.sciencedirect.com
SCIENCE DIRECT®
ELSEVIER
Mutation Research 598 (2006) 120–131
Fundamental and Molecular Mechanisms of Mutagenesis
www.elsevier.com/locate/molmut
Community address: www.elsevier.com/locate/mutres

Molecular mechanisms for maintenance of G-rich short tandem repeats capable of adopting G4 DNA structures

Hitoshi Nakagama*, Kumiko Higuchi, Etsuko Tanaka, Naoto Tsuchiya, Katsuhiko Nakashima, Masato Katahira, Hirokazu Fukuda

Biochemistry Division, National Cancer Center Research Institute, 5-1-1 Tsukiji, Chuo-ku, Tokyo 104-0045, Japan

Available online 2 March 2006

Abstract

Mammalian genomes contain several types of repetitive sequences. Some of these sequences are implicated in various specific cellular events, including meiotic recombination, chromosomal breaks and transcriptional regulation, and also in several human disorders. In this review, we document the formation of DNA secondary structures by the G-rich repetitive sequences that have been found in several minisatellites, telomeres and in various triplet repeats, and report their effects on in vitro DNA synthesis. d(GGCAG) repeats in the mouse minisatellite Pc-1 were demonstrated to form an intra-molecular folded-back quadruplex structure (also called a G4′ structure) by NMR and CD spectrum analyses. d(TTAGGG) telomere repeats and d(CGG) triplet repeats were also shown to form G4′ and other unspecified higher order structures, respectively. In vitro DNA synthesis was substantially arrested within the repeats, and this could be responsible for the preferential mutability of the G-rich repetitive sequences. Electrophoretic mobility shift assays using NIH3T3 cell extracts revealed heterogeneous nuclear ribonucleoprotein (hnRNP) A1 and A3, which were tightly and specifically bound to d(GGCAG) and d(TTAGGG) repeats with K_d values in the order of nM. HnRNP A1 unfolded the G4′ structure formed in the $d(GGCAG)_n$ and $d(TTAGGG)_n$ repeat regions, and also resolved the higher order structure formed by d(CGG) triplet repeats. Furthermore, DNA synthesis arrest at the secondary structures of d(GGCAG) repeats, telomeres and d(CGG) triplet repeats was efficiently repressed by the addition of hnRNP A1. High expression of hnRNPs may contribute to the maintenance of G-rich repetitive sequences, including telomere repeats, and may also participate in ensuring the stability of the genome in cells with enhanced proliferation. Transcriptional regulation of genes, such as *c-myc* and *insulin*, by G4 sequences found in the promoter regions could be an intriguing field of research and help further elucidate the biological functions of the hnRNP family of proteins in human diseases.

Keywords: Molecular mechanism; G4 DNA structure; G-rich repetitive sequence; hnRNPs

1. Introduction

Mammalian genomes are known to contain various types of repetitive sequences, including microsatellites, triplet repeats, minisatellites, and telomeres [1]. LINE, SINE and LTR sequences are also frequently found in the genome of vertebrates [2]. Although there is some variation in the size definition for repeat families, microsatellite repeats are generally composed of short repetitive units of less than 6 nucleotides [1]. It is estimated that more than 100,000 microsatellite loci occur in the mammalian genome. Microsatellites are typically less than 100 base pairs (bp) in total length [3]. Although triplet repeats are also categorized as members of the microsatellite family, some triplet repeat loci can

* Corresponding author. Tel.: +81 3 3547 5239; fax: +81 3 3542 2530.
E-mail address: hnakagam@gan2.res.ncc.go.jp (H. Nakagama).

0027-5107/$ – see front matter © 2006 Elsevier B.V. All rights reserved.
doi:10.1016/j.mrfmmm.2006.01.014

expand to hundreds or even thousands of repeats in certain human disorders (e.g., fragile X syndrome, myotonic dystrophy, Huntington disease) by un-clarified mechanisms [4,5]. In contrast, minisatellite repeats (also known as variable number of tandem repeats; VNTR) are composed of longer repetitive units of 5 or 6–100 nucleotides and are found in arrays expanded up to 10–20 kbp. As opposed to microsatellites, only a few 1000 such loci are present in the genome [6]. Although the biological significance of minisatellite repeats remains largely unknown, some repeat regions are known to be hotspots for meiotic recombination [7,8]. They are also occasionally found in fragile chromosomal sites and could serve as targets for genomic recombination or chromosomal breakage [9,10].

Genetic alteration at a few specific microsatellite and minisatellite repeats results in several human disorders. Alterations in microsatellite repeats are frequently found in cancer cells, and are caused by both genetic and functional alterations of genes encoding mismatch repair proteins, including MLH1, MSH2, MSH6, PMS1, PMS2 and MLH3 [11,12]. Mutations in mismatch repair genes, as occurs in hereditary non-polyposis colorectal cancers, lead to microsatellite instabililty (MSI). MSI can, in turn, cause frame-shift mutations in long tracts of mononucleotides; examples of this have been observed in the transforming growth factor-β type II, BAX and insulin-like growth factor II receptor genes [11,12]. Under mismatch repair-deficient conditions, microsatellite repeats are altered by the insertion or deletion of small numbers of mono- or di-nucleotide repeat units [11,12].

Alteration at certain minisatelllite loci are also implicated in genetic predisposition to some human disorders, such as insulin-dependent diabetes mellitus type 2 (IDDM-2) [13]. A rare allele of the Ha-*ras*-VNTR, which is located in the 3′ region of the Ha-*ras* gene, appears to be associated with various cancers including breast, colon, urinary bladder and acute leukemia [14].

In this review article, characteristic structural features of G-rich short tandem repeats are summarized, and molecular mechanisms involved in maintaining genomic stability at these G-rich repetitive sequences are discussed.

2. Minisatellite Pc-1 and Pc-1-like repeats

The mouse Pc-1 minisatellite (also known as the expanded simple tandem repeat *Ms6-hm*) consists of a tandem array of G-rich repeats $d(GGCAG)_n$, flanked with locus specific sequence [15]. The length of the repeat arrays vary widely among mouse strains [16,17]. Pc-1 was observed to be a recombination hotspot at meiosis, with a germ-line mutation rate as high as 10% per gamete [18,19]. In normal somatic cells, however, the repeats are relatively stable and the mutation rate has been estimated to be around 2×10^{-9} per cell division [17]. To date, many hypervariable minisatellites, consisting of G-rich repeat units similar to Pc-1, have been identified in the mouse and other mammalian genomes. Mouse loci Pc-2 and mo-1 are composed of d(GGCAGG) and d(CTGGGCAGGGAGGA) repeats [16], and human 33.6 and 33.15 minisatellites consist of d(AGGGCTGGAGG) and d(AGAGGTGGGCAGGTGG) repeats, respectively [20]. Since the core sequences of G-rich minisatellites share high similarity among the repeats, more than 20–30 bands are easily detected in mouse and human genomes by a low-stringent DNA fingerprint analysis using Pc-1 as a probe [21,22]. These Pc-1-like repeats are also stable in normal somatic cells, although there are several conditions that can induce mutational instability at this locus [19,21–23].

3. Size alteration of G-rich minisatellite repeats in the genome

Minisatellite repeats are generally stable in somatic cells compared to germ cells as described above [24–26], but alterations at minisatellite regions can be induced both in cell cultures and in vivo [21,27–31]. When culture cells are exposed to a variety of chemical carcinogens, ultraviolet irradiation or ionizing radiation, DNA fingerprint analysis reveals alterations of the banding pattern of genomic regions containing tandem repeats. We hereafter refer to these genetic alterations in minisatellite regions as 'minisatellite mutations', which may include, for example, changes in non-repeat flanking regions and restriction endonuclease sites, deletions/insertions within the repeat regions, and recombination events. Additionally, these types of mutations are frequently observed in sporadic human colorectal and gastric cancers, the incidence being 56% and 25%, respectively [22].

Minisatellite instability is an interesting phenomenon that is suggestive of a novel type of genomic instability [9,23]. As we reported previously, minisatellite instability was observed in a Scid fibroblast cell line transformed by simian virus 40 (SV40) large tumor antigen, SC3VA2, and an embryonal Scid fibroblast cell line, SC1K [23]. Both of these cell lines are deficient in DNA-dependent protein kinase (DNA-PK) activity. A considerable number of size alterations in minisatellites were observed in subclones of both the SC3VA2 and

SC1K cells (45 ± 6% and 37 ± 3%, respectively). These findings were corroborated in several sets of clones. In contrast, cells derived from the RD13B2 cell line, which was established from SC3VA2 by introducing a fragment of the human chromosome 8q, which includes the DNA-PK catalytic subunit, showed a very low frequency of minisatellite mutation (3 ± 3%). Although the underlying molecular mechanisms for this instability have not yet been fully elucidated, a lack of correlation between the presence of minisatellite mutations and microsatellite mutation/instability [21–23] suggests that the mismatch repair system is not involved. Therefore, it appears that another, as yet undiscovered mechanism specific to minisatellite instability, is at play in this case.

4. Formation of G4′ structure by d(GGCAG)$_n$ in vitro

We used structural analyses to investigate whether higher order structures occur in G-rich repetitive sequences to gain further insight into the molecular mechanisms operating in induced instability at these sites. The formation of secondary structures is likely due to the G-rich nature of the repeats. For example, a triple-stranded DNA between d(GGA:TCC) repeats and d(GGA) repeat oligonucleotides forms a D-loop-like higher order structure [32]. The d(CTG:CAG) repeats from the myotonic dystrophy locus form slipped-strand DNA (S-DNA) [33]. A polymorphic G-rich minisatellite, d(ACAGGGGTGTGGGG)$_n$, located in the promoter region of the human insulin gene [34], the G-rich immunoglobulin switch repeats [35], and the G-rich sequence d(G$_{16}$CG(GGT)$_2$GG) in the promoter region of the chicken β-globin gene are also known to form unusual DNA structures, such as four-stranded quadruplexes [36].

Based on these observations, genomic instability at G-rich minisatellites may also be caused as a consequence of the formation of higher order structures of DNA. To investigate this hypothesis, we used the Pc-1 minisatellite repeat, d(GGCAG), as a representative G-rich minisatellite locus of the mouse genome. As shown in Fig. 1A, NMR analysis demonstrated that a synthetic oligonucleotide containing eight repeats of d(GGCAG) (d(GGCAG)$_8$) has the characteristic features necessary to form a quadruplex structure [37]. Circular dichroism (CD) spectrum analysis showed a specific positive CD band at 290–295 nm (Fig. 1B). A positive peak at 260 nm, which is characteristic of the quadruplex with a four-stranded (inter-strand) parallel quadruplex as detailed previously [34,38], was not observed. Furthermore, melting temperatures of oligonucleotides d(GGCAG)$_8$ and d(GGCAG)$_5$ determined by thermal CD melting curves under physiological conditions (100 mM KCl) were independent of DNA concentration. As a reference, a 10-fold dilution of DNA concentration for duplexed DNA causes a 6–8 °C drop of the melting temperature [39]. Taken together, the data indicate that d(GGCAG)$_8$ and d(GGCAG)$_5$ form intra-strand folded-back quadruplex structures (also called a G4′-structure) as opposed to four-stranded quadruplex structures (G4-structure) [37]. The CD spectrum of d(GGCAG)$_3$ was different from those of d(GGCAG)$_5$ and d(GGCAG)$_8$, and gave a broad positive band around 280 nm, but not the typical positive band of the G4′ structure at 290–295 nm (data not shown). Taken together, intra-molecular G:G:G:G tetrad formation with four d(GGG) sequences in d(GGCAG)$_n$

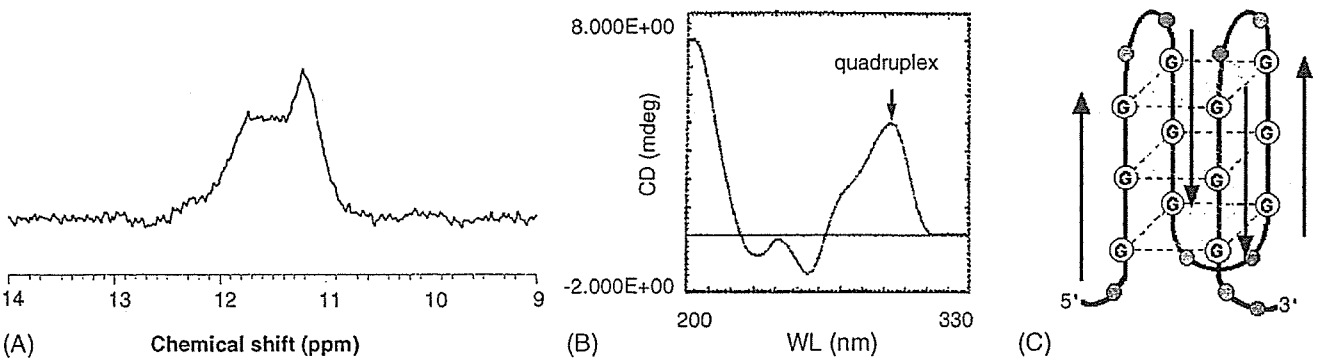

Fig. 1. NMR and CD analysis of d(GGCAG)$_8$ (A) Imino proton NMR spectrum of d(GGCAG)$_8$ in ^2H_2O. The appearance of signals around at 11–12 ppm even in ^2H_2O at 5 °C is characteristic of a quadruplex structure with guanine-quartets. (B) A positive CD band at 290–295 nm is characteristic of a quadruplex with a folded-back structure. A four-stranded parallel quadruplex does not give a positive band at 290–295 nm, but gives one at 260 nm. (C) Schematic diagram illustrating how the d(GGCAG) repeats form a G4′ structure is depicted, although we have not determined yet whether the G4′ structure formed by d(GGCAG) repeats is a "chair" or "basket" type quadruplex [79]. In this model, one G-stretch is aligned anti-parallel to the next G-stretch, and four guanine residues are arranged in a square-planar array.

repeats ($n \geq 5$) could explain the formation of a G4′ structure, as depicted in Fig. 1C.

Although we have not yet proven the in vivo formation of a G4′ structure by d(GGCAG) minisatellite repeats, recent studies by Duquette et al. [40] and Paeschke et al. [41] strongly support the formation of G-quadruplex DNA structures in vivo. Duquette et al. demonstrated the formation of G-loops, novel structures containing G4 DNA, in *E. coli* using plasmid harboring the G-rich regions derived from the mammalian immunoglobulin S (switch) regions and GQN1, an endonuclease that specifically cleaves G4 DNA in the single stranded region 5′ of the stacked G-quartet [42]. Paeschke et al. beautifully demonstrated G-quadruplex formation in the macronucleus of the ciliated *Stylonychia* [41] by the use of antibodies specific for telomeric G-quadruplex DNA [43]. These findings support the hypothesis that G4′ DNA structures form at Pc-1 and Pc-1-like minisatellite repeats in vivo as well. However, further studies are required to validate this hypothesis.

5. DNA synthesis arrest at the d(GGG) sites in vitro

Several studies have demonstrated the ability of d(GGG) sites to cause DNA synthesis arrest. For example, the in vitro DNA synthesis assay showed DNA synthesis arrest at the first d(GGG) site of a single-stranded phagemid (pYA-3) carrying 12 repeats of d(GGCAG), with additional weaker stops at the second, third and fourth d(GGG) sequences (Fig. 2). A primer extension reaction using a synthetic oligonucleotide containing $d(GGCAG)_{15}$ gave similar results (further described below). Inhibition of in vitro DNA synthesis by the formation of G-quadruplex was also reported previously using synthetic oligonucleotides of human [$d(TTAGGG)_n$], the *Tetrahymena* [$d(TTGGGG)_n$] telomeric sequences [44] and the G-rich sequence found in the promoter region of the chicken β-globin gene, $d(G_{16}CG(GGT)_2GG)$ [36,45].

Recently, we found that DNA replication of plasmid in *E. coli* was substantially affected by the presence of d(GGCAG) repeats (unpublished observations). Considering both in vitro and in vivo data, it appears that the presence of the G-rich repeats in the template may inhibit normal DNA synthesis (replication). If this is the case, the lack of repeat instability in somatic cells suggests that somatic cells may have specialized machinery to compensate for the formation of unfavourable higher order DNA structures and to allow replication through the G-rich repeats.

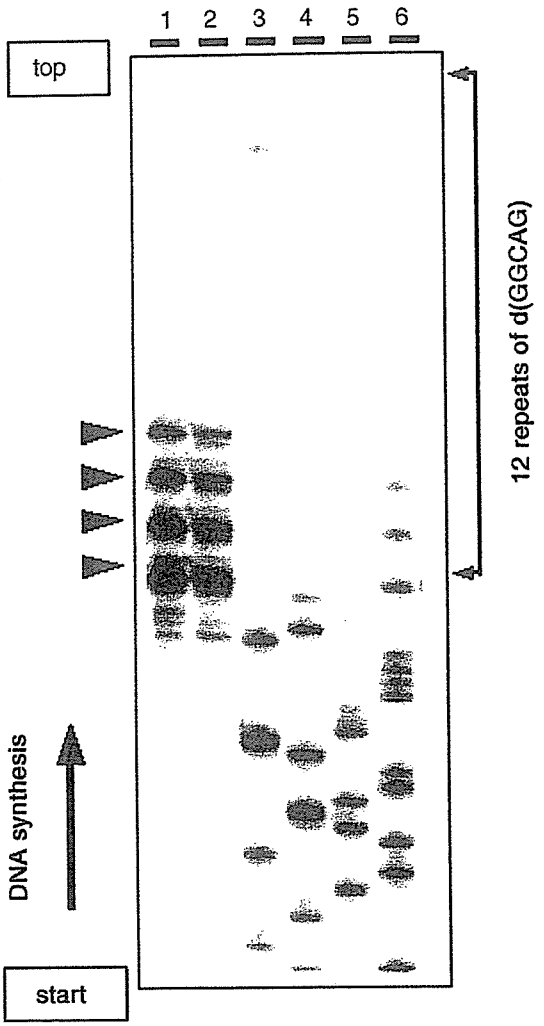

Fig. 2. In vitro DNA synthesis assay using a single-stranded phagemid carrying a $d(GGCAG)_{12}$ repeat. Primer extension reaction was performed as follows using the single-stranded phagemid pYA-3 carrying $d(GGCAG)_{12}$ [37]. The pUC/M13-M4 forward primer (Takara) labeled with ^{32}P at the 5′-end (600 fmol) was annealed with single-stranded pYA-3 (250 fmol) in 5 μl of buffer (40 mM Tris–HCl pH 7.5, 20 mM $MgCl_2$, 50 mM KCl, 5 μM dNTPs) at 72 °C for 5 min, followed by slow cooling to 37 °C. The reaction was started by the addition of 0.5 μl of Sequenase (0.8 U) or the Klenow Fragment (1.0 U), and the mixture was further incubated at 37 °C for 10 min. The reaction was stopped by adding 3.5 μl of the stop solution (10 mM NaOH, 95% formamide, 0.05% bromophenol blue, 0.05% xylene cyanole) and after incubation at 95 °C for 2 min, 3 μl aliquots of the sample DNA were electrophoresed in an 8% polyacrylamide gel containing 7 M urea. Polyacrylamide gel electrophoresis (PAGE) analysis of primer extension reaction with Sequenase (lane 1) or Klenow (lane 2) clearly shows the arrest of in vitro DNA synthesis at the first to fourth d(GGG) sites (arrow heads). Lanes 3–6 show the sequencing reactions with Sequenase in the presence of ddATP, ddTTP, ddCTP and ddGTP, respectively, using 200 fmol of single-stranded pYA-3 plasmids for each reaction. An arrow at the left indicates the direction of DNA synthesis.

6. Isolation of G-rich minisatellite binding proteins

To elucidate the underlying molecular mechanisms for maintenance of genomic stability at genomic G-

Table 1
Isolation of minisatellite binding proteins from NIH3T3 cell extract [48]

ID	MW (kDa)	Common name
MNBP-A	30	hnRNP A3
MNBP-B	24	hnRNP A1/UP1
MNBP-D	29	ND[a]
MNBP-E	98	LRP130[b]
MNBP-F	130	LRP130
MNBP-G	110	Tudor-SN/SND1

[a] ND: not determined.
[b] Probably a proteolytic product of MNBP-F, LRP130.

rich minisatellite sequences, we carried out an electrophoretic mobility shift assay (EMSA) to identify minisatellite binding proteins (MNBPs) using cell-free extracts from NIH3T3 cells treated with okadaic acid (Table 1). Okadaic acid (OA) is a known tumor promoter [46] and a specific inhibitor of the mammalian serine/threonine protein phosphatases [47]. OA is capable of inducing minisatellite mutations in NIH3T3 cells [21]. Two proteins, hnRNP A3 (MNBP-A) and hnRNP A1 (MNBP-B), were identified from OA-treated NIH3T3 cells as MNBPs for the G-rich strand of the Pc-1 minisatellite [48]. In addition, three proteins, MNBP-D, LRP130 (MNBP-E and -F) and Tudor-SN/SND1 (MNBP-G), were identified as C-rich strand binding proteins [48], whose functions and biological consequences will be briefly discussed later.

Binding of hnRNP A1 in cell-free extracts to the G-rich repeat was enhanced from cultures treated with 5 nM of OA. In contrast, hnRNP A3 did not show any such enhancement after OA treatment, suggesting some mechanistic differences in DNA recognition and binding between the two hnRNPs. Sequence requirements for the high-binding affinity of hnRNP A1 and hnRNP A3 were evaluated by an oligonucleotide competition assay using EMSA, and are summarized in Table 2. hnRNP A1 binds more widely to $d(GGCAG)_5$ and d(GGCAG)-like repeats, including $G5_{TEL}$, $G5_{+T}$ and poly(dG), with a K_d value of nM magnitudes. Interestingly, the affinity of hnRNA3 with $d(GGCAG)_5$ was about 50-fold weaker than that of hnRNP A1, with IC_{50} values for the formation of $d(GGCAG)_8$-protein complexes being 300 and 6 nM, respectively (see footnote for Table 2). This suggests that tandem arrays ($n > 5$ units) are required for sufficient binding of hnRNP A3 with Pc-1 $d(GGCAG)_n$ repeats. In contrast, competition with telomere repeats ($G5_{TEL}$) and telomere-like repeats ($G5_{+T}$) showed much stronger inhibitory activity for hnRNP A3 binding to $d(GGCAG)_8$, the value of which was almost comparable to that observed for hnRNP A1. $G5_{Pc\text{-}2}$, which contains a G-insertion in the d(GGCAG) repeat of Pc-1, and is similar to minisatellite Pc-2, showed a slightly lower binding activity than the d(GGCAG) repeats. $G5_{+C}$ did not bind to either hnRNP A1 or hnRNP A3. A large difference was also observed between hnRNP A1 and hnRNP A3 with poly (dG) probes. Binding of hnRNP A3 to poly(dG) was 100-fold weaker than hnRNP A1.

Table 2
IC_{50} values for formation of $d(GGCAG)_8$–protein complexes with hnRNP A1, hnRNP A3 and UP1 [48,52]

Competitor	hnRNP A1	hnRNP A3	UP1
$G5_{TEL}$ ($(GTTAGG)_5$)	3 nM	5 nM	3 nM
$G5_{+T}$ ($(GTCAGG)_5$)	1 nM	7 nM	4 nM
$G5_{Pc\text{-}2}$ ($(GGCAGG)_5$)	9 nM	20 nM	40 nM
G5 ($(GGCAG)_5$)	6 nM	300 nM	20 nM
Poly(dG) ($(dG)_{25}$)	9 nM	1 μM	100 nM
$G5_{+C}$ ($(GCCAGG)_5$)	>1 μM	>1 μM	>1 μM

IC_{50} values were estimated from the inhibition curves generated by plotting the relative amount of complex against the concentration of a competitor, and expressed as the concentrations of individual unlabeled competitor oligonucletides at which the labeled $d(GGCAG)_8$–protein complex yield was halved. The concentration of labeled $d(GGCAG)_8$ used in the competition reaction is 2 nM in all experiments.

Based on our data, minisatellite Pc-1 binding proteins are able to bind not only to Pc-1 but also to other minisatellites having Pc-1-like sequences. Sequence requirements for DNA binding of hnRNP A3 seem to be stricter than those for hnRNP A1, and this suggests that hnRNP A3 may serve a different function from hnRNP A1 by binding to separate regions of the genome. Both hnRNP A1 and hnRNP A3 may be telomere binding proteins, and elucidation of the biological functions of hnRNP A3 is currently ongoing in our laboratory.

7. hnRNP A1 and UP1 bind to G-rich repetitive sequences and unfold G4′ structures

To clarify the consequence of hnRNP A1 binding to G-rich repetitive sequences, we investigated its effect on the stability of the G4′ structure. Recombinant hnRNP A1 and unwinding protein 1 (UP1), a proteolytic product of hnRNP A1 lacking the C-terminal portion of hnRNP A1 [49–51], were expressed in *E. coli* as GST fusion proteins and purified, by releasing a GST tag, for use in G4′ binding assays. DNA binding affinity and sequence specificity of UP1 is almost equivalent to those of GST-UP1 and GST-hnRNP A1, but is slightly lower than that of hnRNP A1 (Table 2).

By EMSA, the intramolecular quadruplex (G4′ form) of $d(GGCAG)_8$ shows faster mobility than the single-stranded form on polyacrylamide gel electrophoresis (PAGE). Both UP1 and GST-hnRNP A1 bind to both

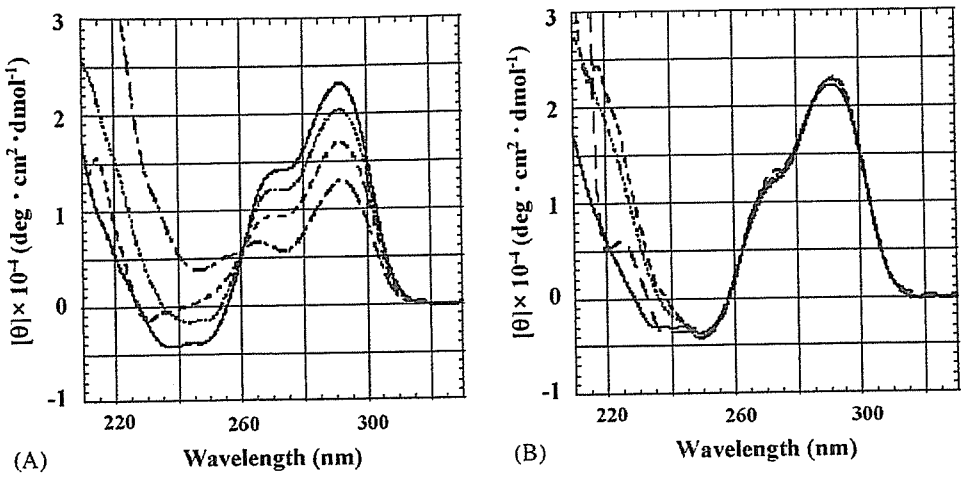

Fig. 3. CD spectra indicate UP1 unfolds the G4′ structure of d(GGCAG) repeats. CD spectra of $d(GGCAG)_5$ with GST-UP1 (A) and GST (B). For each CD spectrum, the spectrum of the corresponding protein was subtracted. Solid, the DNA:protein molar ratio of 1:0; dotted, 1:0.5; dashed, 1:1; centered, 1:2. The CD band at 290–295 nm was decreased by addition of GST-UP1 in a dose-dependent manner. GST alone did not induce any change in the levels of the peak.

G4′ and single-stranded forms of $d(GGCAG)_8$ [52], and decrease, in a dose dependent manner, the amount of the G4′ form (unpublished data). The characteristic CD band at 290–295 nm of the G4′ structure was decreased by addition of GST-UP1 in a concentration-dependent manner (Fig. 3A), while the addition of GST did not induce any change (Fig. 3B). These data clearly indicate that hnRNP A1 and UP1 unfold the G4′ structure at the d(GGCAG) repeats.

Another member of the hnRNP family proteins, hnRNP D, also binds and destabilizes the quadruplex structure formed by telomeric $d(TTAGGG)_n$ repeats, and is suggested to be involved in maintenance of the telomere 3′-overhang [53]. LR1, a heterodimer of nucleolin and hnRNP D, binds to duplex DNA sites in the immunoglobulin heavy chain switch (S) regions, which are G-rich DNA regions conforming to the consensus sequence, dGGNCNAG(G/C)CTG(G/A) [54]. Dempsey et al. demonstrated LR1 binding to G4 DNA formed by G-G pairing in S region sequences, and suggested that LR1 may juxtapose donor and acceptor switch regions for recombination during S region transcription [54]. Two hnRNP-related telomeric DNA-binding proteins, uqTBP25 and qTBP42, which show close sequence similarity to hnRNP A1, hnRNP A2/B1 and/or hnRNP C, also bind to quadruplex telomeric DNA and increase the heat stability and resistance of the telomeric repeats to micrococcal nuclease digestion [55,56]. Weisman-Shomer et al. recently demonstrated that both uqTBP25 and qTBP42 destabilize the quadruplex (tetraplex) structures of $d(CGG)_n$, but quadruplex structures of telomeric and IgG sequences are resistant to destabilization by these two proteins, suggesting the presence of some structural differences among the quadruplexes [57].

8. Abrogation of DNA synthesis arrest at the G4′ structure by UP1

When template carrying $d(GGCAG)_{12}$ was used for an in vitro DNA synthesis assay, a primer extension reaction with *BcaBEST* DNA polymerase was obstructed mainly at the first d(GGG) site (Fig. 4A). A primer extension reaction with a synthetic oligonucleotide containing a $d(CAGGG)_{15}$ repeat also demonstrated that progression of DNA polymerase was obstructed mainly at the first d(GGG) site followed by additional weaker stops at the second, third, fourth, fifth and sixth d(GGG) sites (Fig. 4B). When UP1 was added to the reaction with an excess molar amount over the template, DNA synthesis arrest at the d(GGG) sites was reduced in a dose-dependent manner and the synthesis of the complete length of template DNA was considerably enhanced (Fig. 4A and B). Other DNA polymerases, such as Taq, Klenow fragment and human DNA polymerase α (pol α) also gave similar results [52]. The data suggest that UP1/hnRNP A1 may abrogate DNA synthesis arrests at d(GGG) sites by destabilizing the G4′ structure. UP1 does not require NTP hydrolysis energy to unfold the quadruplex as, for example, BLM and WRN helicases do to unwind tetra- or bi-molecular quadruplex DNA [58,59].

9. Destruction of the telomere G4′ structure by binding of UP1

UP1 also binds to $G5_{+TEL}$ and TRM4 $[d(TTAGGG)_4]$, both of which contain four telomeric repeats [52,60]. Under physiological-like conditions, $d(TTAGGG)_4$ also gave a positive CD band at

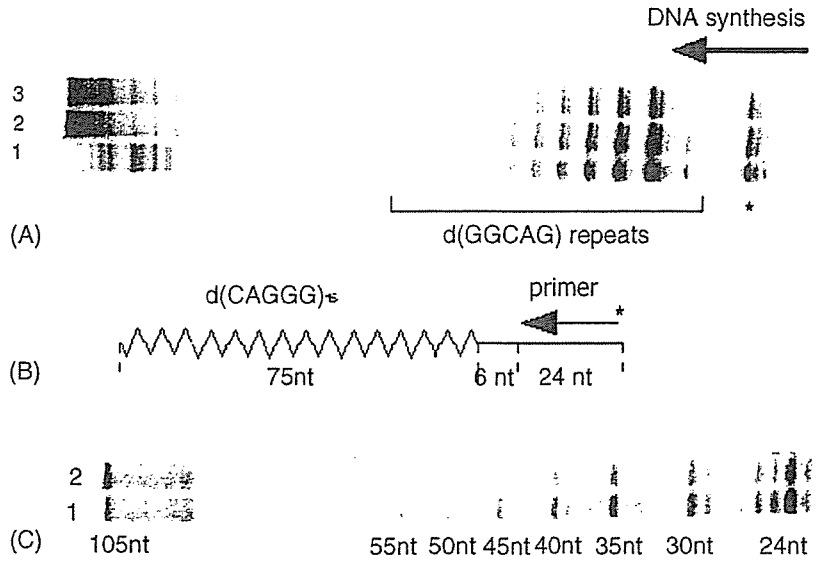

Fig. 4. Effect of UP1 on the arrest of DNA synthesis at d(GGCAG) repeats. (A) Denaturing PAGE analysis of primer extension reactions was carried out with or without UP1 using the single-stranded phagemid pYA-3 carrying $d(GGCAG)_{12}$ as described above (see legend of Fig. 2.) with some modifications [52]. *BcaBEST* DNA polymerase was used for the reaction. Single-stranded pYA-3 with $d(GGCAG)_{12}$ repeat (final 100 nM) in TE buffer containing 100 mM KCl was stored at 7 °C overnight to allow sufficient formation of the quadruplex structure, after heat denaturation at 95 °C for 3 min. Five μl of DNA samples was mixed with 7.5 μl of Milli-Q water and 5 μl of the pUC/M13 (−40) forward primer (Promega) labeled with ^{32}P at the 5′-end (0.5 μM) in TE buffer. The mixture was heated at 60 °C for 7 min and incubated at 37 °C for more than 30 min to allow sufficient quadruplex formation. An aliquot of 1.75 μl of this primer-annealed template (final 23 nM) was mixed with 0.75 μl of 10× *BcaBEST* buffer (200 mM Tris–HCl, pH 8.5/100 mM $MgCl_2$) and 0.5 μl of dNTPs mixture (50 μM each). After addition of 4 μl GST-UP1 suspended in a reaction buffer (20 mM sodium phophate, pH 7.0/0.5 mM DTT), the mixture was incubated at 37 °C for 5 min, and then the primer extension reaction was carried out at 37 °C for 8 min in the presence of *BcaBEST* DNA polymerase (final 66 units/ml). Final concentrations of UP1 added in the reaction are 0 M (lane 1), 6.0 μM (lane 2) and 48 μM (lane 3), respectively. Horizontal arrows indicate the direction of the DNA synthesis, and an asterisk (*) indicates the pausing of the primer extension at d(GGG) present in the multiple cloning sites of the vector plasmid. (B) and (C) A primer extension reaction using a synthetic oligonucleotide pSub15 as a template was performed in the presence and absence of GST-UP1 as described above with some modification. A schematic representation of a 105-mer template pSub15 with $d(CAGGG)_{15}$ repeats used for the primer extension reaction is depicted (B). A mixture of the pSub15 and ^{32}P-labeled M13–20 (Takara) primer (final 100 nM each) was heated in TE buffer containing 150 mM KCl at 95 °C for 5 min and then at 72 °C for 5 min, followed by gradual cooling to room temperature, and stored at 7 °C overnight. The concentrations of *BcaBEST* DNA polymerase, the primer-annealed template, and dNTPs were 18 units/ml, 10 nM, and 1.7 μM, respectively. The concentrations of GST-UP1 were 0 M (lane 1 in (C)) and 750 nM (lane 2 in (C)). Fragment sizes are indicated in nucleotides (nt).

290–295 nm, similar to d(GGCAG) repeats, indicating the formation of a G4′ structure [52]. In contrast, four-stranded parallel quadruplex DNA was not observed except at a much higher DNA concentration (data not shown). In vitro DNA synthesis using synthetic oligonucleotides and several DNA polymerases, including human pol α, was also strongly inhibited at the d(GGG) sites of the telomeric repeats (our unpublished observation). The CD band at 290–295 nm, which is specific for the G4′ structure, was also decreased by addition of GST-UP1 in a dose-dependent manner as in the case of the d(GGCAG) repeats. GST alone did not induce any change in the levels of the band peak [52].

In hnRNP A1-deficient cells, telomere repeats become significantly shorter than in cells with normal levels of hnRNP A1 expression [61]. Restoration of hnRNP A1 expression dramatically increased the average size of the terminal repeat fragment length of the telomere. Interaction of telomerase with hnRNP A1 was also demonstrated by LaBranche et al. [61]. Physical interaction of hnRNP A1, telomeric DNA and human telomerase RNA was also demonstrated by Fiset and Chabot in vitro [62]. These results suggest that hnRNP A1 and its shortened derivative UP1 possibly play a key role in telomere maintenance by destroying the quadruplex structure of the telomere end in vivo. After destruction of the G4′ structure of telomere repeats, telomeric regions may become accessible for telomerase binding, enabling the proper maintenance of telomeres in cells [63].

10. UP1 unfolds the higher order DNA structures of d(CGG) triplet repeats

Another important functional aspect of UP1 is its role in the unfolding the higher order DNA structures of d(CGG) triplet repeats [64]. The $d(CGG)_n$ tract

forms hairpin, quadruplex, and homoduplex structures in vitro under physiological-like conditions [64–66]. In our study, the CD band analysis of $d(CGG)_{16}$ in either the presence or absence of 150 mM KCl showed a large negative peak at 255 nm and a weak positive peak at 280 nm, suggesting the formation of a non-B-type higher order DNA structure (Fig. 5A). The CD spectrum of oligonucleotide CGG16mut, having C to A substitutions at two sites in CGG16, represented a typical pattern of the B structure with comparable negative and positive peaks at 255 and 280 nm, respectively (Fig. 5B). Fragile X syndrome, the most common form of inherited mental retardation in humans, is caused by expansion of a d(CGG) triplet repeat in the 5′-untranslated region of the first exon of the FMR1 gene [67–69]. Although the molecular mechanisms underlying the unstable expansion of the repeats are yet to be elucidated, formation of higher order DNA structures by d(CGG) repeats as described above could be responsible for the induction of genomic instability and the expansion mutation at these repeats.

Several proteins have been identified and reported to unfold or destabilize the higher order structure of $d(CGG)_n$, including WRN helicase [59,70] and two telomeric DNA binding proteins, qTBP42 and uqTBP25 [57]. Here, we demonstrate that UP1 also

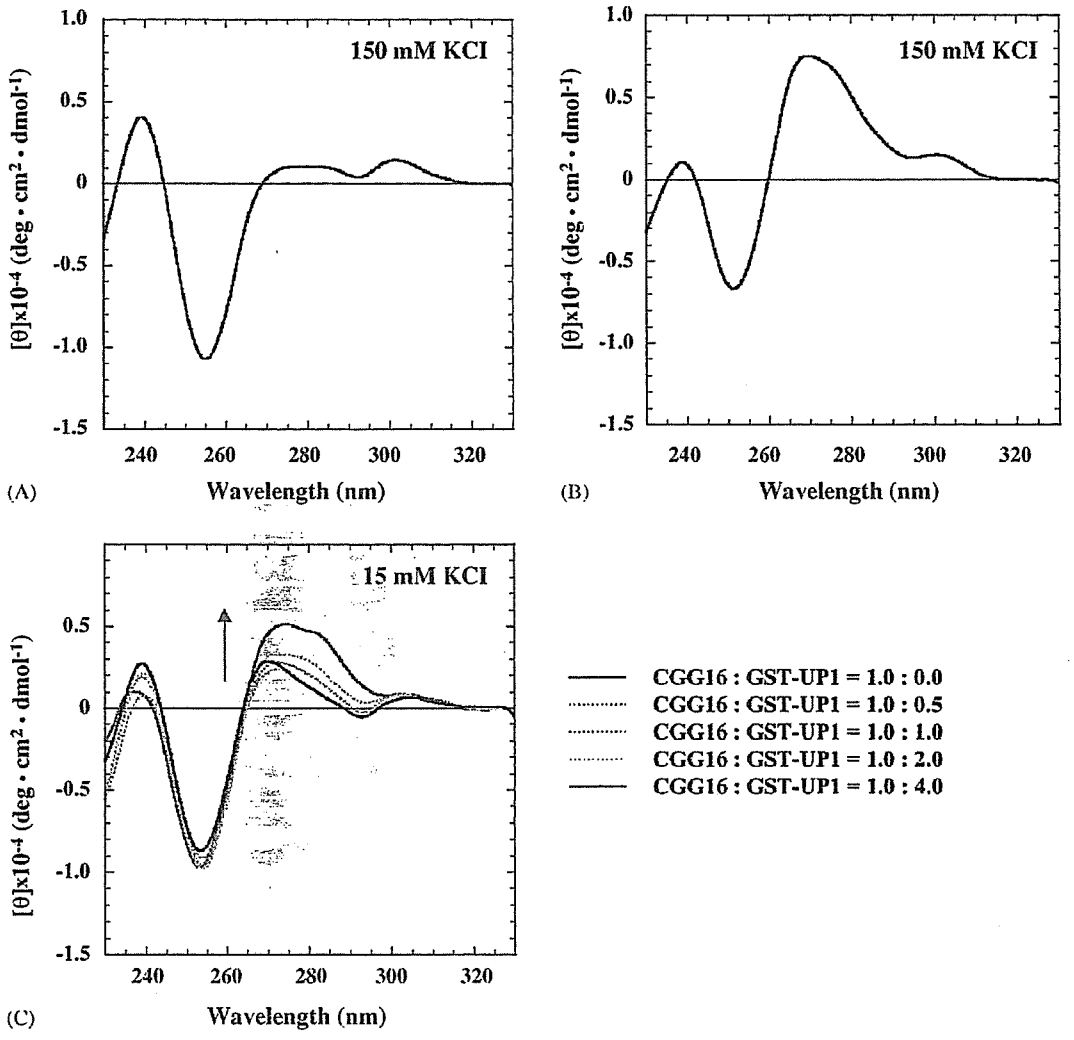

Fig. 5. CD spectra showing the effect of UP1 on higher order DNA structures of the d(CGG) repeat. (A) CD spectrum of $d(CGG)_{16}$ [CGG16] in the presence of 150 mM KCl. A large negative peak at 255 nm and a weak positive peak at 280 nm, which is suggestive of the formation of a non-B-type DNA structure, was observed. CGG16 also gave a similar CD pattern in the absence of KCl (data not shown). (B) CD spectrum of oligonucleotide CGG16mut in the presence of 150 mM KCl. CGG16mut, the sequence being $d(CGG)_5(AGG)(CGG)_4(AGG)(CGG)_5$, has C to A substitutions at two sites in CGG16. The spectrum represents a typical pattern of the B-structure with comparable negative and positive peaks at 255 and 280 nm, respectively. CGG16mut also showed the B-structure pattern in the absence of KCl. (C) CD spectra of CGG16 titrated with GST-UP1 in the presence of 15 mM KCl, the concentration at which the primer extension reaction was carried out with a synthetic 92-mer oligonucleotide pSubCGG16, containing a d(CGG) repeat, as a template. From each spectrum, the spectrum of the corresponding protein is subtracted, and CGG16:GST-UP1 molar ratios are indicated at the right bottom. Arrows indicate the changes of positive peaks of CD spectra in accordance with increased amounts of added GST-UP1 protein.

binds and unfolds the non-B structure of d(CGG) repeats (Fig. 5C). DNA synthesis is severely obstructed in vitro within the repetitive sequence, similar to the d(GGCAG)$_n$ repeats (data not shown). Addition of molar excess (compared to the template) of GST-UP1 reduces the arrest of DNA synthesis for several DNA polymerases in vitro, including human DNA polymerase α [64].

11. Expression of hnRNP A1 and hnRNP A3 in sporadic human colorectal cancers

Both hnRNP A1 and A3 are over-expressed in human colorectal cancers [71]. In the case of hnRNP A1, quantitative gene expression analysis revealed that 60% (18/30) of sporadic human colorectal cancers showed over-expression of hnRNP A1 in cancer tissues by at least two-fold compared to their normal counterparts. Interestingly, 78% of cases at clinicopathological stage II showed increased expression of two-fold or greater; this is two-fold higher than that seen in the more advanced stage IV [71]. This may imply that the biological impact of hnRNP A1 over-expression is in the relatively early stages of colon carcinogenesis. The over-expression of hnRNP A1 could contribute to the maintenance of telomere repeats in cancer cells and allow enhanced cell proliferation.

12. C-rich strands of minisatellite binding proteins

C-rich binding proteins, LRP130 and Tudor-SN/SND1, were also isolated from OA-treated NIH3T3 cells using oligonucleotide d(CTGCC)$_8$ as a probe, as described earlier [48]. It has been demonstrated that LRP130 and Tudor-SN/SND1 have some sequence specificity for DNA binding [72,73]. Interestingly, both LRP130 and Tudor-SN/SND1 bind to C-rich RNA sequences in a sequence specific manner, and are mainly localized at perinuclear regions and in the cytoplasm [74]. This may suggest the involvement of LRP130 and Tudor-SN/SND1 in RNA metabolism, mRNA transportation and/or specific mRNA transcription of sequences harboring a portion of C-rich residues. At present, we do not have a clear idea of the biological functions of these C-rich DNA/RNA binding proteins. It is possible that these proteins cooperate with hnRNP A1 and A3 (that bind to the G-rich DNA sequences) and exert some novel control of, for example, transcriptional regulation, mRNA metabolism or some other biological pathways.

13. Implication of G4 DNA structures in promoter regions in gene transcription

Although the biological roles of G-rich repeat sequences capable of adopting G4 DNA structures are still largely elusive, one of the intriguing fields of G4 DNA structure research is in its possible involvement in regulation of gene transcription. The G4′-quadruplex structure of the promoter region of the *c-myc* oncogene has been found to function as a transcriptional repressor [75] and the expression of *c-myc* can be inhibited by ligand-mediated G4-quadruplex stabilization [76]. In the case of the human insulin gene, unusual DNA structures of 14 bp G-rich tandem repeats are also thought to affect transcriptional activity, possibly through formation of G-quartets [34,77]. The presence of a guanine-quadruplex forming region within a polypurine tract of the hypoxia inducible factor 1α (HIF1α) promoter was also recently demonstrated; this unusual DNA structure may be involved in regulation of basal HIF-1α expression [78].

14. Future perspectives

G-rich repetitive sequences are frequently observed in the genome and are a subset of triplet repeats and of minisatellite DNA. Because of the peculiar and specific DNA structures adopted by G-rich repetitive sequences, these genomic regions might induce DNA replication fork arrest, leading to size alterations of the repeats in vivo. Various cellular components, such as WRN, TBPs, UP1 and hnRNP A1, may work as guardians against G-rich repeat length instability. In addition, C-rich sequence binding proteins, LRP130 and Tudor-SN/SND1, may cooperate with G-rich binding proteins, and facilitate the resolution of G4′ structures. A fascinating and intriguing scenario for the biological function of these MNBPs is their involvement in transcription of either the G- or C-rich repeat strands. Indeed, most MNBPs isolated from NIH3T3 cells in our own studies as well as by others, bind to mRNA transcripts (data not shown). Binding of hnRNP A1 and hnRNP A3 to G- or C-rich transcripts may affect the transcriptional efficiency and/or the fate of the transcripts of the G-rich region in the genome [40]. Further studies should be conducted to gain more insight into the biological impact of G-rich repetitive sequences, which are widely spread throughout the genome.

Acknowledgements

The authors thank Drs. Minako Nagao and Takashi Sugimura for their helpful comments and continuing

upport for the research. This work was supported by Grant-in-Aid for Cancer Research from the Ministry f Health, Labour and Welfare of Japan, and Grants-in-id for Scientific Research (for M.K. and for H.F.) and he Protein 3000 Project (for M.K.) from the Ministry f Education, Culture, Sports, Science and Technology f Japan. K.H., E.T. and K.N. are the recipients of a esearch Resident Fellowship from the Foundation for romotion of Cancer Research in Japan.

eferences

[1] J.C. Venter, M.D. Adams, E.W. Myers, P.W. Li, R.J. Mural, G.G. Sutton, H.O. Smith, M. Yandell, C.A. Evans, R.A. Holt, The sequence of the human genome, Science 291 (2001) 1304–1351.

[2] M. Dewannieux, T. Heidmann, LINEs, SINEs and processed pseudogenes: parasitic strategies for genome modeling, Cytogenet. Genome Res. 110 (2005) 35–48.

[3] H. te Riele, N. Claij, Microsatellite instability in human cancer: a prognostic marker for chemotherapy, Exp. Cell Res. 246 (1999) 1–10.

[4] C.J. Cummings, H.Y. Zoghbi, Fourteen and counting: unraveling trinucleotide repeat diseases, Hum. Mol. Genet. 9 (2000) 909–916.

[5] N.A. Di Prospero, K.H. Fishbeck, Therapeutics development for triplet repeat expansion diseases, Nat. Rev. Genet. 6 (2005) 756–765.

[6] A.J. Jeffreys, M.J. Allen, J.A.L. Armour, A. Collick, Y. Dubrova, N. Fretwell, T. Guram, M. Jobling, C.A. May, D.L. Neil, R. Neumann, Mutation processes at human minisatellites, Electrophoresis 16 (1995) 1577–1585.

[7] W.P. Wahls, L.J. Wallace, P.D. Moore, Hypervariable minisatellite DNA is a hotspot for homologous recombination in human cells, Cell 60 (1990) 95–103.

[8] A.J. Jeffreys, J.K. Holloway, L. Kauppi, C.A. May, R. Neumann, M.T. Slingsby, A.J. Webb, Meiotic recombination hot spots and human DNA diversity, Philos. Trans. R. Soc. London B: Biol. Sci. 359 (2004) 141–152.

[9] O. Handt, G.R. Sutherland, R.I. Richards, Fragile sites and minisatellite repeat instability, Mol. Genet. Metab. 70 (2000) 99–105.

[10] S. Yu, M. Mangelsdorf, D. Hewett, L. Hobson, E. Baker, H.J. Eyre, N. Lapsys, D. Le Paslier, N.A. Doggett, G.R. Sutherland, R.I. Richards, Human chromosomal fragile site FRA16B is an amplified AT-rich minisatellite repeat, Cell 88 (1997) 367–374.

[11] A. de la Chapelle, Genetic predisposition to colorectal cancer, Nat. Rev. Cancer 4 (2004) 769–780.

[12] P. Peltomaki, Deficient DNA mismatch repair: a common etiologic factor for colon cancer, Hum. Mol. Genet. 10 (2001) 735–740.

[13] T.G. Krontiris, Minisatellites and human disease, Science 269 (1995) 1682–1683.

[14] T.G. Krontiris, B. Devlin, D.D. Karp, N.J. Robert, N. Risch, An association between the risk of cancer and mutations in the HRAS1 minisatellite locus, N. Engl. J. Med. 329 (1993) 517–523.

[15] R. Kelly, G. Bulfield, A. Collick, M. Gibbs, A.J. Jeffreys, Characterization of a highly unstable mouse minisatellite locus: evidence for somatic mutation during early development, Genomics 5 (1989) 844–856.

[16] K. Mitani, Y. Takahashi, R. Kominami, A GGCAGG motif in minisatellites affecting their germline instability, J. Biol. Chem. 265 (1990) 15203–15210.

[17] S. Suzuki, K. Mitani, K. Kuwabara, Y. Takahashi, O. Niwa, R. Kominami, Two mouse hypervariable minisatellites: chromosomal location and simultaneous mutation, J. Biochem. (Tokyo) 114 (1993) 292–296.

[18] M.N. Weitzmann, K.J. Woodford, K. Usdin, The mouse Ms6-hm hypervariable microsatellite forms a hairpin and two unusual tetraplexes, J. Biol. Chem. 273 (1998) 30742–30749.

[19] M. Yamauchi, M. Nishimura, S. Tsuji, M. Terada, M. Sasanuma, Y. Shimada, Effect of SCID mutation on the occurrence of mouse Pc-1 (Ms6-hm) germline mutations, Mutat. Res. 503 (2002) 43–49.

[20] A.J. Jeffreys, V. Wilson, S.L. Thein, Hypervariable 'minisatellite' regions in human DNA, Nature 314 (1985) 67–73.

[21] H. Nakagama, S. Kaneko, H. Shima, H. Inamori, H. Fukuda, R. Kominami, T. Sugimura, M. Nagao, Induction of minisatellite mutation in NIH 3T3 cells by treatment with the tumor promoter okadaic acid, Proc. Natl. Acad. Sci. U.S.A. 94 (1997) 10813–10816.

[22] H. Inamori, S. Takagi, R. Tajima, M. Ochiai, T. Ubagai, T. Sugimura, M. Nagao, H. Nakagama, Frequent and multiple mutations at minisatellite loci in sporadic human colorectal and gastric cancers—possible mechanistic differences from microsatellite instability in cancer cells, Jpn. J. Cancer Res. 93 (2002) 382–388.

[23] H. Imai, H. Nakagama, K. Komatsu, T. Shiraishi, H. Fukuda, T. Sugimura, M. Nagao, Minisatellite instability in severe combined immunodeficiency mouse cells, Proc. Natl. Acad. Sci. U.S.A. 94 (1997) 10817–10820.

[24] Y.E. Dubrova, Long-term genetic effects of radiation exposure, Mutat. Res. 544 (2003) 433–439.

[25] A.J. Jeffreys, K. Tamaki, A. MacLeod, D.G. Monckton, D.L. Neil, J.A. Armour, Complex gene conversion events in germline mutation at human minisatellites, Nat. Genet. 6 (1994) 136–145.

[26] C.L. Yauk, Advances in the application of germline tandem repeat instability for in situ monitoring, Mutat. Res. 566 (2004) 169–182.

[27] T. Kitazawa, R. Kominami, R. Tanaka, K. Wakabayashi, M. Nagao, 2-Hydroxyamino-1-methyl-6-phenylimidazo[4,5-*b*]pyridine induction of recombinational mutations in mammalian cell lines as detected by DNA fingerprinting, Mol. Carcinogr. 9 (1994) 67–70.

[28] B.J. Ledwith, D.J. Joslyn, P. Troilo, K.R. Leander, J.H. Clair, K.A. Soper, S. Manam, S. Prahalada, M.J. van Zwieten, W.W. Nichols, Induction of minisatellite DNA rearrangements by genotoxic carcinogens in mouse liver tumors, Carcinogenesis 16 (1995) 1167–1172.

[29] B.J. Ledwith, R.D. Storer, S. Prahalada, S. Manam, K.R. Leander, M.J. van Zwieten, W.W. Nichols, M.O. Bradley, DNA fingerprinting of 7,12-dimethylbenz[*a*]anthracene-induced and spontaneous CD-1 mouse liver tumors, Cancer Res. 50 (1990) 5245–5249.

[30] Y. Matsumura, D. Tarin, DNA fingerprinting survey of various human tumors and their metastases, Cancer. Res. 52 (1992) 2174–2179.

[31] S.L. Thein, A.J. Jeffreys, H.C. Gooi, F. Cotter, J. Flint, N.T. O'Connor, D.J. Weatherall, J.S. Wainscoat, Detection of somatic changes in human cancer DNA by DNA fingerprint analysis, Br. J. Cancer 55 (1987) 353–356.

[32] Y. Mishima, T. Suda, R. Kominami, Formation of a triple-stranded DNA between d(GGA:TCC) repeats and d(GGA) repeat oligonucleotides, J. Biochem. (Tokyo) 119 (1996) 805–810.

[33] C.E. Pearson, Y.H. Wang, J.D. Griffith, R.R. Sinden, Structural analysis of slipped-strand DNA (S-DNA) formed in $(CTG)_n$. $(CAG)_n$ repeats from the myotonic dystrophy locus, Nucl. Acids Res. 26 (1998) 816–823.
[34] P. Catasti, X. Chen, R.K. Moyzis, E.M. Bradbury, G. Gupta, Structure–function correlations of the insulin-linked polymorphic region, J. Mol. Biol. 264 (1996) 534–545.
[35] D. Sen, W. Gilbert, Formation of parallel four-stranded complexes by guanine-rich motifs in DNA and its implications for meiosis, Nature 334 (1988) 364–366.
[36] K.J. Woodford, R.M. Howell, K. Usdin, A novel K(+)-dependent DNA synthesis arrest site in a commonly occurring sequence motif in eukaryotes, J. Biol. Chem. 269 (1994) 27029–27035.
[37] M. Katahira, H. Fukuda, H. Kawasumi, T. Sugimura, H. Nakagama, M. Nagao, Intramolecular quadruplex formation of the G-rich strand of the mouse hypervariable minisatellite Pc-1, Biochem. Biophys. Res. Commun. 264 (1999) 327–333.
[38] P. Balagurumoorthy, S.K. Brahmachari, D. Mohanty, M. Bansal, V. Sasisekharan, Hairpin and parallel quartet structures for telomeric sequences, Nucl. Acids Res. 20 (1992) 4061–4067.
[39] M. Katahira, M. Kanagawa, H. Sato, S. Uesugi, S. Fujii, T. Kohno, T. Maeda, Formation of sheared G:A base pairs in an RNA duplex modelled after ribozymes, as revealed by NMR, Nucl. Acids Res. 22 (1994) 2752–2759.
[40] M.L. Duquette, P. Handa, J.A. Vincent, A.F. Taylor, N. Maizels, Intracellular transcription of G-rich DNAs induces formation of G-loops, novel structures containing G4 DNA, Genes Dev. 18 (2004) 1618–1629.
[41] K. Paeschke, T. Simonsson, J. Postberg, D. Rhodes, H.J. Lipps, Telomere end-binding proteins control the formation of G-quadruplex DNA structures in vivo, Nat. Struct. Mol. Biol. 12 (2005) 847–854.
[42] H. Sun, A. Yabuki, N. Maizels, A human nuclease specific for G4 DNA, Proc. Natl. Acad. Sci. U.S.A. 98 (2001) 12444–12449.
[43] C. Schaffitzel, I. Berger, J. Postberg, J. Hanes, H.J. Lipps, A. Pluckthun, In vitro generated antibodies specific for telomeric guanine-quadruplex DNA react with Stylonychia lemnae macronuclei, Proc. Natl. Acad. Sci. U.S.A. 98 (2001) 8572–8577.
[44] H. Han, L.H. Hurley, M. Salazar, A DNA polymerase stop assay for G-quadruplex-interactive compounds, Nucl. Acids Res. 27 (1999) 537–542.
[45] R.M. Howell, K.J. Woodford, M.N. Weitzmann, K. Usdin, The chicken beta-globin gene promoter forms a novel "cinched" tetrahelical structure, J. Biol. Chem. 271 (1996) 5208–5214.
[46] M. Suganuma, H. Fujiki, H. Suguri, S. Yoshizawa, M. Hirota, M. Nakayasu, M. Ojika, K. Wakamatsu, K. Yamada, T. Sugimura, Okadaic acid: an additional non-phorbol-12-tetradecanoate-13-acetate-type tumor promoter, Proc. Natl. Acad. Sci. U.S.A. 85 (1988) 1768–1771.
[47] A. Takai, C. Bialojan, M. Troschka, J.C. Ruegg, Smooth muscle myosin phosphatase inhibition and force enhancement by black sponge toxin, FEBS Lett. 217 (1987) 81–84.
[48] H. Fukuda, T. Sugimura, M. Nagao, H. Nakagama, Detection and isolation of minisatellite Pc-1 binding proteins, Biochim. Biophys. Acta 1528 (2001) 152–158.
[49] G. Herrick, B. Alberts, Purification and physical characterization of nucleic acid helix-unwinding proteins from calf thymus, J. Biol. Chem. 251 (1976) 2124–2132.
[50] B.M. Merrill, M.B. LoPresti, K.L. Stone, K.R. Williams, High pressure liquid chromatography purification of UP1 and UP2, two related single-stranded nucleic acid-binding proteins from calf thymus, J. Biol. Chem. 261 (1986) 878–883.
[51] O. Valentini, G. Biamonti, M. Pandolfo, C. Morandi, S. Riva, Mammalian single-stranded DNA binding proteins and heterogeneous nuclear RNA proteins have common antigenic determinants, Nucl. Acids Res. 13 (1985) 337–346.
[52] H. Fukuda, M. Katahira, N. Tsuchiya, Y. Enokizono, T. Sugimura, M. Nagao, H. Nakagama, Unfolding of quadruplex structure in the G-rich strand of the minisatellite repeat by the binding protein UP1, Proc. Natl. Acad. Sci. U.S.A. 99 (2002) 12685–12690.
[53] Y. Enokizono, Y. Konishi, K. Nagata, K. Ouhashi, S. Uesugi, F. Ishikawa, M. Katahira, Structure of hnRNP D complexed with single-stranded telomere DNA and unfolding of the quadruplex by heterogeneous nuclear ribonucleoprotein D, J. Biol. Chem. 280 (2005) 18862–18870.
[54] L.A. Dempsey, H. Sun, L.A. Hanakahi, N. Maizels, G4 DNA binding by LR1 and its subunits, nucleolin and hnRNP D, A role for G–G pairing in immunoglobulin switch recombination, J. Biol. Chem. 274 (1999) 1066–1071.
[55] R. Erlitzki, M. Fry, Sequence-specific binding protein of single-stranded and unimolecular quadruplex telomeric DNA from rat hepatocytes, J. Biol. Chem. 272 (1997) 15881–15890.
[56] G. Sarig, P. Weisman-Shomer, R. Erlitzki, M. Fry, Purification and characterization of qTBP42, a new single-stranded and quadruplex telomeric DNA-binding protein from rat hepatocytes, J. Biol. Chem. 272 (1997) 4474–4482.
[57] P. Weisman-Shomer, Y. Naot, M. Fry, Tetrahelical forms of the fragile X syndrome expanded sequence d(CGG)(*n*) are destabilized by two heterogeneous nuclear ribonucleoprotein-related telomeric DNA-binding proteins, J. Biol. Chem. 275 (2000) 2231–2238.
[58] H. Sun, J.K. Karow, I.D. Hickson, N. Maizels, The Bloom's syndrome helicase unwinds G4 DNA, J. Biol. Chem. 273 (1998) 27587–27592.
[59] M. Fry, L.A. Loeb, Human werner syndrome DNA helicase unwinds tetrahelical structures of the fragile X syndrome repeat sequence $d(CGG)_n$, J. Biol. Chem. 274 (1999) 12797–12802.
[60] Y. Enokizono, A. Matsugami, S. Uesugi, H. Fukuda, N. Tsuchiya, T. Sugimura, M. Nagao, H. Nakagama, M. Katahira, Destruction of quadruplex by proteins, and its biological implications in replication and telomere maintenance, Nucl. Acids Res. Suppl. (2003) 231–232.
[61] H. LaBranche, S. Dupuis, Y. Ben-David, M.R. Bani, R.J. Wellinger, B. Chabot, Telomere elongation by hnRNP A1 and a derivative that interacts with telomeric repeats and telomerase, Nat. Genet. 19 (1998) 199–202.
[62] S. Fiset, B. Chabot, hnRNP A1 may interact simultaneously with telomeric DNA and the human telomerase RNA in vitro, Nucl. Acids Res. 29 (2001) 2268–2275.
[63] L.P. Ford, W.E. Wright, J.W. Shay, A model for heterogeneous nuclear ribonucleoproteins in telomere and telomerase regulation, Oncogene 21 (2002) 580–583.
[64] H. Fukuda, M. Katahira, E. Tanaka, Y. Enokizono, N. Tsuchiya, K. Higuchi, M. Nagao, H. Nakagama, Unfolding of higher DNA structures formed by the d(CGG) triplet repeat by UP1 protein, Genes Cells 10 (2005) 953–962.
[65] M. Fry, L.A. Loeb, The fragile X syndrome $d(CGG)_n$ nucleotide repeats form a stable tetrahelical structure, Proc. Natl. Acad. Sci. U.S.A. 91 (1994) 4950–4954.
[66] P. Fojtik, I. Kejnovska, M. Vorlickova, The guanine-rich fragile X chromosome repeats are reluctant to form tetraplexes, Nucl. Acids Res. 32 (2004) 298–306.

7] D.C. Crawford, J.M. Acuna, S.L. Sherman, FMR1 and the fragile X syndrome: human genome epidemiology review, Genet. Med. 3 (2001) 359–371.
8] J.L. Mandel, Questions of expansion, Nat. Genet. 4 (1993) 8–9.
9] F. Rousseau, D. Heitz, J.L. Mandel, The unstable and methylatable mutations causing the fragile X syndrome, Hum. Mutat. 1 (1992) 91–96.
0] A.S. Kamath-Loeb, L.A. Loeb, E. Johansson, P.M. Burgers, M. Fry, Interactions between the Werner syndrome helicase and DNA polymerase delta specifically facilitate copying of tetraplex and hairpin structures of the d(CGG)$_n$ trinucleotide repeat sequence, J. Biol. Chem. 276 (2001) 16439–16446.
1] M. Ushigome, T. Ubagai, H. Fukuda, N. Tsuchiya, T. Sugimura, J. Takatsuka, H. Nakagama, Up-regulation of hnRNP A1 gene in sporadic human colorectal cancers, Int. J. Oncol. 26 (2005) 635–640.
2] H. Fukuda, N. Tsuchiya, M. Sato, A. Yamaguchi, N. Tanaka, M. Nagao, H. Nakagama, DNA-binding activity of p100, a transcriptional coactivator, to single-stranded C-rich sequences, Proc. Jpn. Acad. 79 (Ser(B)) (2003) 120–123.
3] N. Tsuchiya, H. Fukuda, T. Sugimura, M. Nagao, H. Nakagama, LRP130, a protein containing nine pentatricopeptide repeat motifs, interacts with a single-stranded cytosine-rich sequence of mouse hypervariable minisatellite Pc-1, Eur. J. Biochem. 269 (2002) 2927–2933.
[74] N. Tsuchiya, H. Fukuda, K. Nakashima, M. Nagao, T. Sugimura, H. Nakagama, LRP130, a single-stranded DNA/RNA-binding protein, localizes at the outer nuclear and endoplasmic reticulum membrane, and interacts with mRNA in vivo, Biochem. Biophys. Res. Commun. 317 (2004) 736–743.
[75] T. Simonsson, P. Pecinka, M. Kubista, DNA tetraplex formation in the control region of c-myc, Nucl. Acids Res. 26 (1998) 1167–1172.
[76] T. Lemarteleur, D. Gomez, R. Paterski, E. Mandine, P. Mailliet, J.F. Riou, Stabilization of the c-myc gene promoter quadruplex by specific ligands' inhibitors of telomerase, Biochem. Biophys. Res. Commun. 323 (2004) 802–808.
[77] A. Lew, W.J. Rutter, G.C. Kennedy, Unusual DNA structure of the diabetes susceptibility locus IDDM2 and its effect on transcription by the insulin promoter factor Pur-1/MAZ, Proc. Natl. Acad. Sci. U.S.A. 97 (2000) 12508–12512.
[78] R. De Armond, S. Wood, D. Sun, L.H. Hurley, S.W. Ebbinghaus, Evidence for the presence of a guanine quadruplex forming region within a polypurine tract of the hypoxia inducible factor 1alpha promoter, Biochemistry 44 (2005) 16341–16350.
[79] V.M. Marathias, P.H. Bolton, Determinants of DNA quadruplex structural type: sequence and potassium binding, Biochemistry 38 (1999) 4355–4364.

Available online at www.sciencedirect.com
SCIENCE DIRECT®
Cancer Letters 241 (2006) 87–92
CANCER Letters
www.elsevier.com/locate/canlet

Parp-1 deficiency does not increase the frequency of tumors in the oral cavity and esophagus of ICR/129Sv mice by 4-nitroquinoline 1-oxide, a carcinogen producing bulky adducts

Akemi Gunji [a,b], Akiko Uemura [a,c], Masahiro Tsutsumi [d], Tadashige Nozaki [a], Osamu Kusuoka [d], Ken Omura [b,e], Hiroshi Suzuki [f], Hitoshi Nakagama [a], Takashi Sugimura [a], Mitsuko Masutani [a,c,*]

[a] *Biochemistry Division, National Cancer Center Research Institute, 5-1-1, Tsukiji, Chuo-ku, Tokyo 104-0045, Japan*
[b] *Department of Oral Surgery, Tokyo Medical and Dental University Graduate School, Bunkyo-ku, Tokyo, Japan*
[c] *ADP-ribosylation in Oncology Project, National Cancer Center Research Institute, 5-1-1, Tsukiji, Chuo-ku, Tokyo 104-0045, Japan*
[d] *Department of Oncological Pathology, Cancer Center, Nara Medical University, 840, Shijo-cho, Kashihara, Nara 634-8521, Japan*
[e] *Department of Advanced Molecular Diagnosis and Maxillofacial Surgery, Hard Tissue Genome Research Center, Tokyo Medical and Dental University*
[f] *Chugai Pharmaceutical Co. Ltd. Gotemba, 1-135, Komakado, Gotemba, Shizuoka, 412-0038, Japan*

Received 28 July 2005; received in revised form 2 October 2005; accepted 7 October 2005

Abstract

The impact of poly(ADP-ribose) polymerase-1 (*Parp−1*)-deficiency on 4-nitroquinoline 1-oxide (4NQO)-induced carcinogenesis was studied in mice with an ICR/129Sv mixed genetic background. *Parp-1*$^{+/+}$, *Parp−1*$^{+/-}$ and *Parp-1*$^{-/-}$ animals given 4NQO for thirty-two weeks at 0.001% in their drinking water developed papillomas and squamous cell carcinomas of the tongue, palate and esophagus, but with no statistically significant variation with the *Parp−1* genotype. Thus *Parp-1* deficiency does not elevate susceptibility to carcinogenesis induced by a carcinogen which gives rise to bulky DNA lesions. This study also indicated that the ICR/129Sv mixed genetic background is associated with high yield induction of esophageal tumors by 4NQO.

Keywords: 4-Nitroquinoline 1-oxide; Poly(ADP-ribose) polymerase-1; Squamous cell carcinoma; Carcinogenesis; Knockout mice

1. Introduction

Poly(ADP-ribose) polymerase (Parp)-1 is activated by DNA strand breaks and polyADP-ribosylates various nuclear proteins, including itself and histones, using NAD as a substrate [1,2]. Accumulated evidence indicates that Parp−1 is involved in base excision repair (BER) as well as repair of single- and double-strand breaks [3–6] and *Parp-1*$^{-/-}$ mice are generally more susceptible than their *Parp−1*$^{+/+}$ counterparts to carcinogenic activity of alkylating agents [7,8]. Incidences of tumors have also been found to be augmented in SCID*Parp-1*$^{-/-}$ [5] and *Ku80*$^{+/-}$ *Parp−1*$^{-/-}$ [9] as compared with *Parp-1*$^{+/+}$ mice, in good accordance with the accepted role of Parp−1 in BER and DNA strand break repair.

* Corresponding author. Address: ADP-ribosylation in Oncology Project, National Cancer Center Research Institute, 1-1, Tsukiji 5-chome, Chuo-ku, Tokyo 104-0045, Japan. Tel.: +81 3 3542 2511x4551; fax: +81 3 3542 2530.
E-mail address: mmasutan@gan2.res.ncc.go.jp (M. Masutani).

0304-3835/$ - see front matter © 2006 Elsevier Ireland Ltd. All rights reserved.
doi:10.1016/j.canlet.2005.10.003

While, it is postulated that Parp-1 does not contribute to nucleotide excision repair (NER) [10], the main pathway for repair of bulky DNA lesions, its involvement in cell death accompanying NAD depletion [6,11,12] and also in the maintenance of genomic stability [13–15] as well as control of differentiation [16–18], suggest that *Parp*$-1^{-/-}$ mice might be susceptible to carcinogenesis by all types of carcinogens, independent of the type of DNA adducts that they generate. However, in contrast to the high susceptibility to carcinogenesis induced by alkylating agents in *Parp-1*$^{-/-}$ mice, tumor yields in response to a heterocyclic amine, 2-amino-3-methylimidazo[4,5-*f*]quinoline (IQ), which produces bulky DNA adducts, were not elevated in the lungs and liver [19]. To further clarify the impact of *Parp*-1 deficiency on carcinogenesis induced by different types of carcinogens, we here employed 4-nitroquinoline 1-oxide (4NQO) [20], which give rises to DNA adducts that may be mainly repaired through NER like UV-induced DNA lesions [21], in a mice strain with a mixed genetic background of 129Sv/ICR.

2. Materials and methods

2.1. Mice

Parp-1$^{+/-}$ and *Parp*$-1^{-/-}$ mice used in this study were generated by disrupting the *Parp-1* exon 1 through the insertion of a neomycin resistance gene cassette as described previously [22]. *Parp*$-1^{+/+}$, *Parp*$-1^{+/-}$ and *Parp*$-1^{-/-}$ male mice with a mixed genetic background of ICR/129Sv were produced by brother–sister mating of *Parp*$-1^{+/-}$ mice [22]. Genotypes were determined by Southern blot analysis using tail-tip DNA samples as described elsewhere [22]. The animals were housed in plastic cages in an air-conditioned room with a 12 h light–dark cycle and basal diet (CE-2, CLEA JAPAN, Tokyo, Japan) and sterilized water were available *ad libitum*. The experimental protocol was approved by the Ethics Review Committees for Animal Experimentation of the participating institutions.

2.2. Carcinogenesis experiment

4NQO (Sigma) was dissolved and diluted with sterilized drinking water to achieve a concentration of 0.001% and administered orally *ad libitum* from light-shielded polyvinyl bottles for 32 weeks, starting at the age of 9 weeks. The bottles were changed with fresh 4NQO solution once a week and consumption was recorded to estimate the intake of 4NQO. Five each of the *Parp*$-1^{+/+}$, *Parp*$-1^{+/-}$ and *Parp*$-1^{-/-}$ mice were used as controls and fifteen *Parp*$-1^{+/+}$, eighteen *Parp*$-1^{+/-}$ and eleven *Parp*$-1^{-/-}$ mice served for 4NQO treatment. Body weights of the mice were measured once a week. At 32 weeks after the initiation of 4NQO administration, mice were anesthetized with ether and autopsies were performed. All organs were examined macroscopically for the presence of tumors and the tongue, esophagus and stomach were fixed in neutralized 10% formalin solution and routinely processed for embedding in paraffin. For the palate and nasal cavity, decalcification was performed with formic acid/formalin fixation. Sections were cut at 3 μm thickness and stained with hematoxylin and eosin (HE) for histopathological analysis.

2.3. Statistical analysis

The χ^2 analysis and Fisher's exact tests were performed to compare data for incidences and the Student-*t* test and Wilcoxon-Mann-Whitney-U test for the body weights, 4NQO intake and multiplicities of the tumors, using SSPS software on Macintosh computers.

3. Results

Three *Parp*$-1^{-/-}$ mice demonstrated loss of condition and were subjected to autopsy at 29 or 31 weeks after initiation of 4NQO administration, all harbouring tumors in either the oral cavity or the esophagus. The experiment was therefore terminated at 32 weeks and autopsy was performed for the remaining animals. There were no significant differences in the initial mean body weights among the genotypes (Table 1). At the end of experiment, an apparent increase of body weights was observed in *Parp*$-1^{+/+}$ and *Parp*$-1^{+/-}$ mice of the 4-NQO-treated ($P=0.76$ and $P<0.005$, respectively) and untreated groups ($P=0.008$ and $P=0.007$, respectively) but not in *Parp*$-1^{-/-}$ mice. The values for *Parp*$-1^{+/-}$ mice were slightly higher than those for *Parp*$-1^{-/-}$ mice in both 4-NQO-treated and untreated groups ($P=0.034$ and $P=0.008$, respectively), but the values for 4-NQO-treated *Parp*$-1^{+/+}$ and *Parp*$-1^{-/-}$ mice were not statistically different. Total intake of 4NQO did not significantly differ among the *Parp*-1 genotypes (data not shown).

As summarized in Tables 2 and 3, tumors were observed in the oral cavity, esophagus and stomach after 4NQO administration in animals of each genotype, but not in the control groups. One *Parp*$-1^{+/-}$ mouse given

Table 1
Initial and final body weights

Group	*Parp-1*	4NQO (0.001%)	Effective no. of mice	Initial body weight (g)[a]	Final body weight (g)[a]
1	+/+	+	15	31.0±0.7	34.5±1.7
2	+/−	+	18	31.7±0.9	36.8±1.9[b]
3	−/−	+	11	31.2±0.9	33.7±1.3[c, d]
4	+/+	−	5	29.6±0.5	37.1±1.2[e]
5	+/−	−	5	32.3±1.0	42.5±1.5[d, e]
6	−/−	−	5	32.9±2.3	33.6±0.9[f]

[a] Mean+SE.
[b] Significantly different from the initial body weight (at $P<0.0001$).
[c] Three mice were subjected to autopsy before the termination of experiment and mean body weight of the remaining mice at thirty-two weeks was measured.
[d] Significantly different from the final body weight of the *Parp*$-1^{+/-}$ group given 4NQO (at $p<0.05$).
[e] Significantly different from the initial body weight (at $P<0.01$).
[f] Significantly different from the final body weight of the untreated *Parp*$-1^{+/-}$ group (at $P<0.01$).

4NQO developed a tumor in the Harderian glands. Tumors in the oral cavity were mainly observed in the tongue, as in *XPA*$^{-/-}$ mice with the C57BL/6 genetic background [23], but also in the palate but not the nasal cavity. There were no significant differences in the incidences, multiplicities or histology of hyperplasia, papillomas and squamous cell carcinomas (SCCs) in the oral cavity among the *Parp*-1 genotypes.

High incidences of hyperplasia and papillomas, and to a lesser extent SCCs, were also observed in the esophagus of *Parp*$-1^{+/+}$ mice as well as other genotypes, again with no statistically significant influence of the *Parp*-1 genotype. In the stomach, two *Parp*$-1^{+/+}$ mice harboured a papilloma and an SCC and hyperplasia was observed in one *Parp*$-1^{-/-}$ mouse.

4. Discussion

The present study demonstrated no variation in susceptibility to 4NQO carcinogenicity among *Parp*$-1^{+/+}$, *Parp*$-1^{+/-}$ and *Parp*$-1^{-/-}$ mice. Because the incidences of papillomas and SCCs in the oral cavity and of SCCs in the esophagus were relatively low, the absence of any differences in the incidences was not due to a saturation dose of 4NQO. We also recently found that the susceptibility to carcinogenesis induced by a heterocyclic amine, IQ, did not differ between *Parp*$-1^{+/+}$ and *Parp*$-1^{-/-}$ mice with a C57BL/6 genetic background [19]. It is known that genetic background can affect the outcome of carcinognenesis experiments but our previous results showed increased susceptibility of the same

Table 2
Incidences and multiplicities of tumors in the oral cavity

	Parp-1	4NQO (0.001%)	Effective no.of mice	Tongue			Palate		
				Hyperplasia	Papilloma	SCC[a]	Hyperplasia	Papilloma	SCC[a]
Incidences[b]									
Control	+/+	(−)	5	0	0	0	0	0	0
	+/−	(−)	5	0	0	0	0	0	0
	−/−	(−)	5	0	0	0	0	0	0
4NQO	+/+	(+)	15	9 (56)	5 (33)	3 (20)	6 (40)	1 (6)	0
	+/−	(+)	18	6 (33)	4 (22)	1 (6)	11 (61)	1 (5)	0
	−/−	(+)	11	6 (55)	2 (18)	1 (9)	7 (63)	2 (18)	2 (18)
Multiplicity[c]									
4NQO	+/+	(+)	15	1.3±0.2	1.4±0.3	1.0	1.3±0.2	2.0	0
	+/−	(+)	18	1.3±0.2	1.3±0.3	1.0	1.6±0.2	1.0	0
	−/−	(+)	11	1.3±0.2	1.0±0	1.0	1.6±0.3	1.0	1.0

[a] Squamous cell carcinoma.
[b] No. of mice bearing tumor (%).
[c] No. of tumors per mouse bearing tumor. Mean (when no. of tumors was one) or mean±SE (when no. of tumors was greater than two).

Table 3
Incidences and multiplicities of tumors in the esophagus and stomach

	Parp-1	4NQO (0.001%)	Effective no.of mice	Esophagus			Stomach		
				Hyperplasia	Papilloma	SCC[a]	Hyperplasia	Papilloma	SCC[a]
Incidences[b]									
Control	+/+	(−)	5	0	0	0	0	0	0
	+/−	(−)	5	0	0	0	0	0	0
	−/−	(−)	5	0	0	0	0	0	0
4NQO	+/+	(+)	15	11 (73)	9 (60)	2 (13)	0	1 (7)	1 (7)
	+/−	(+)	18	13 (72)	13 (72)	6 (33)	0	0	0
	−/−	(+)	11	8 (73)	9 (82)	1 (9)	1 (9)	0	0
Multiplicity[c]									
	+/+	(+)	15	3.9±0.7	4.7±0.9	1.0	0	1.0	1.0
	+/−	(+)	18	3.4±0.5	3.8±0.9	1.3±0.2	0	0	0
	−/−	(+)	11	3.9±0.4	3.6±0.9	2.0	1.0	0	0

[a] Squamous cell carcinoma.
[b] No. of mice bearing tumor (%).
[c] No. of tumors per mouse bearing tumor. Mean (when no. of tumors was two) or mean±SE (when no. of tumors was greater than two).

Parp$-1^{-/-}$ 129Sv/ICR mice to carcinogenesis induced by alkylating agents [7,8]. The data therefore strongly support our current view that the suppressive role of Parp-1 is limited to particular types of carcinogens, dependent on the repair pathway for individual carcinogen-induced lesions.

4NQO is reduced by nitroreductase [24] or DT diaphorase [25] to a proximate carcinogen, 4-hydroxyquinoline-1-oxide (4HQO), which binds to serine residues in aminoacyl-tRNA synthetase to generate the ultimate carcinogen [26] producing adducts on the N-2 and C-8 positions of guanine residues as well as the N-6 position of adenine residues [27]. 4NQO induces mutations in the bone marrow, lungs and livers as well as in the stomach when administered by gavage [28]. Transversion mutations at guanine residues parallel the amounts of C-8 adducts on guanine residues [29] as well as transition mutations at guanine residues [30], these being mainly repaired by NER like DNA adducts induced by IQ [21]. In the NER pathway, global genome repair, transcription-coupled repair (TCR) and translesion synthesis are known as the major components. Eighty-six and zero percent of *XPA*$^{-/-}$ and *XPA*$^{+/+}$ mice, respectively, were found to develop tongue tumors after administration of 0.001% 4NQO in drinking water for 50 weeks, implying that global genome repair or TCR involving the XPA protein may be important for the removal of lesions induced by 4NQO. In contrast, DNA lesions induced by alkylating agents, such as BHP and azoxymethane, are mainly repaired by base-excision repair (BER), alkylguanine alkyltransferases, DNA strand break repair or homologous recombination repairs (HRR). Therefore, our results support the notion that Parp-1 plays a role in the suppression of carcinogenesis due to alkylation-induced DNA damage, but not through the NER pathway.

4NQO also increases the frequency of chromosomal aberrations [31] and micronucleus formation [32], suggesting that DNA strand breaks could also be induced through oxidative stress [33]. We here terminated the experiment at 32 weeks from the initiation of 4NQO administration because animals bearing tumors were observed from 29 weeks. On the other hand, there are significant differences in the final body weights among the genotypes. *Parp-1*$^{-/-}$ mice of both untreated and 4NQO treated groups did not show gain of body weight, in contrast to *Parp-1*$^{+/+}$ and *Parp-1*$^{+/-}$ mice. 4NQO administration reduced the gain of body weight in *Parp-1*$^{+/-}$ mice, whereas those of *Parp-1*$^{+/+}$ and *Parp-1*$^{-/-}$ mice were apparently unaffected by 4NQO. The results suggest that 4NQO toxicity might be possibly slightly different among the three genotypes. Therefore, it may be of interest to carry out a longer term experiment using a lower dose of 4NQO to further evaluate the susceptibility to carcinogenesis in *Parp-1*-deficient mice.

Certain nitrosamines, such as benzylmethylnitrosamine and phenylmethylnitrosamine, are known to induce high yields of esophageal tumors in rodents [34]. Steidler et al. reported that when 4NQO was applied repeatedly to the palates of male CBA mice, only 20% developed papillomas or SCCs in the esophagus after 12–16 weeks treatment [35]. We unexpectedly found that our mice with an ICR/129SV mixed genetic background are highly susceptible to

esophageal tumor development induced by 4NQO. The same concentration of 0.001% 4NQO in drinking water administered to the C57BL/6 strain did not result in the generation of esophageal tumors as previously reported [23]. Therefore, the ICR/129SV mouse strain may be particularly useful for studies of the carcinogenic actions of 4NQO.

In conclusion, we demonstrated here that the susceptibility to 4NQO-induced carcinogenesis in the oral cavity and esophagus is not altered by *Parp−1* deficiency.

Acknowledgements

We appreciate the suggestions provided by Sakae Tatematsu. We are grateful to Kazuyoshi Yanagihara for maintenance of the animals and Atsushi Shibata and Hisako Fujihara for technical assistance. This work was supported in part by a Grant-in-Aid for Cancer Research from the Ministry of Health, Labour and Welfare of Japan and a Grant-in-Aid for Scientific Research from the Ministry of Education, Science, Sports, and Culture of Japan (13771123).

References

[1] T. Sugimura, Poly(adenosine diphosphate ribose), Prog. Nucleic Acid Res. Mol. Biol. 13 (1973) 127–151.
[2] A. Burkle, V. Schreiber, F. Dantzer, F.J. Oliver, C. Niedergang, G. de Murcia, J. Menissier-de Murcia, Biological significance of poly(ADP-ribosyl)ation reactions: molecular and genetic approaches, in: G. de Murcia, S. Shall (Eds.), From DNA Damage and Stress Signaling to Cell Death. PolyADP-ribosylation Reactions, Oxford University Press, New York, 2000, pp. 80–124.
[3] C. Trucco, F.J. Oliver, G. de Murcia, J. Menissier-de Murcia, DNA repair defect in poly(ADP-ribose) polymerase-deficient cell lines, Nucleic Acids Res. 26 (1998) 2644–2649.
[4] F. Dantzer, V. Schreiber, C. Niedergang, C. Trucco, E. Flatter, G. de La Rubia, et al., Involvement of poly(ADP-ribose) polymerase in base excision repair, Biochimie 81 (1999) 69–75.
[5] C. Morrison, G.C. Smith, L. Stingl, S.P. Jackson, E.F. Wagner, Z.Q. Wang, Genetic interaction between PARP and DNA-PK in V(D)J recombination and tumorigenesis, Nat. Genet. 17 (1997) 479–482.
[6] S.W. Yu, H. Wang, M.F. Poitras, C. Coombs, W.J. Bowers, H.J. Federoff, et al., Mediation of poly(ADP-ribose) polymerase-1-dependent cell death by apoptosis-inducing factor, Science 297 (2002) 259–263.
[7] M. Tsutsumi, M. Masutani, T. Nozaki, O. Kusuoka, T. Tsujiuchi, H. Nakagama, et al., Increased susceptibility of poly(ADP-ribose) polymerase-1 knockout mice to nitrosamine carcinogenicity, Carcinogenesis 22 (2001) 1–3.
[8] T. Nozaki, H. Fujihara, M. Watanabe, M. Tsutsumi, K. Nakamoto, O. Kusuoka, et al., Parp-1 deficiency implicated in colon and liver tumorigenesis induced by azoxymethane, Cancer Sci. 94 (2003) 497–500.
[9] W.M. Tong, U. Cortes, M.P. Hande, H. Ohgaki, L.R. Cavalli, P.M. Lansdorp, et al., Synergistic role of Ku80 and poly(ADP-ribose) polymerase in suppressing chromosomal aberrations and liver cancer formation, Cancer Res. 62 (2002) 6990–6996.
[10] Z.Q. Wang, B. Auer, L. Stingl, H. Berghammer, D. Haidacher, M. Schweiger, E.F. Wagner, Mice lacking ADPRT and poly(ADP-ribosyl)ation develop normally but are susceptible to skin disease, Genes Dev. 9 (1995) 509–520.
[11] H. Yamamoto, Y. Uchigata, H. Okamoto, Streptozotocin and alloxan induce DNA strand breaks and poly(ADP-ribose) synthetase in pancreatic islets, Nature 294 (1981) 284–286.
[12] N.A. Berger, Poly(ADP-ribose) in the cellular response to DNA damage, Radiat. Res. 101 (1985) 4–15.
[13] R. Ding, M. Smulson, Depletion of nuclear poly(ADP-ribose) polymerase by antisense RNA expression: influences on genomic stability, chromatin organization, and carcinogen cytotoxicity, Cancer Res. 54 (1994) 4627–4634.
[14] J.M. De Murcia, C. Niedergang, C. Trucco, M. Ricoul, B. Dutrillaux, M. Mark, et al., Requirement of poly(ADP-ribose) polymerase in recovery from DNA damage in mice and in cells, Proc. Natl Acad. Sci. USA 94 (1997) 7303–7307.
[15] Z.Q. Wang, L. Stingl, C. Morrison, M. Jantsch, M. Los, K. Schulze-Osthoff, E.F. Wagner, PARP is important for genomic stability but dispensable in apoptosis, Genes Dev. 11 (1997) 2347–2358.
[16] Y. Ohashi, K. Ueda, O. Hayaishi, K. Ikai, O. Niwa, Induction of murine teratocarcinoma cell differentiation by suppression of poly(ADP-ribose) synthesis, Proc. Natl Acad. Sci. USA 81 (1984) 7132–7136.
[17] T. Nozaki, M. Masutani, M. Watanabe, T. Ochiya, F. Hasegawa, H. Nakagama, et al., Syncytiotrophoblastic giant cells in teratocarcinoma-like tumors derived from *Parp*-disrupted mouse embryonic stem cells, Proc. Natl Acad. Sci. USA 96 (1999) 13345–13350.
[18] M.E. Smulson, V.H. Kang, J.M. Ntambi, D.S. Rosenthal, R. Ding, C.M. Simbulan, Requirement for the expression of poly(ADP-ribose) polymerase during the early stages of differentiation of 3T3-L1 preadipocytes, as studied by antisense RNA induction, J. Biol. Chem 270 (1995) 119–127.
[19] K. Ogawa, M. Masutani, K. Kato, M. Tang, N. Kamada, H. Suzuki, et al., Parp-1 deficiency does not enhance liver carcinogenesis induced by 2-amino-3-methylimidazo[4,5-f] quinoline in mice, Cancer Lett, in press.
[20] W. Nakahara, F. Fukuoka, T. Sugimura, Carcinogenic action of 4-nitroquinoline-N-oxide, Gan 48 (1957) 129–137.
[21] M. Ikenaga, Y. Ishii, M. Tada, T. Kakunaga, H. Takebe, Excision-repair of 4-nitroquinolin-1-oxide damage responsible for killing, mutation, and cancer, Basic Life Sci. 5B (1975) 763–771.
[22] M. Masutani, H. Suzuki, N. Kamada, M. Watanabe, O. Ueda, T. Nozaki, et al., Poly(ADP-ribose) polymerase gene disruption conferred mice resistant to streptozotocin-induced diabetes, Proc. Natl Acad. Sci. USA 96 (1999) 2301–2304.
[23] F. Ide, H. Oda, Y. Nakatsuru, K. Kusama, H. Sakashita, K. Tanaka, T. Ishikawa, Xeroderma pigmentosum group A gene action as a protection factor against 4-nitroquinoline 1-oxide-induced tongue carcinogenesis, Carcinogenesis 22 (2001) 567–572.
[24] A.M. Benson, Conversion of 4-nitroquinoline 1-oxide (4NQO) to 4-hydroxyaminoquinoline 1-oxide by a dicumarol-resistant hepatic 4NQO nitroreductase in rats and mice, Biochem. Pharmacol. 46 (1993) 1217–1221.
[25] T. Sugimura, K. Okabe, M. Nagao, The metabolism of 4-nitroquinoline-1-oxide, a carcinogen. 3. an enzyme catalyzing

the conversion of 4-nitroquinoline-1-oxide to 4-hydroxyaminoquinoline-1-oxide in rat liver and hepatomas, Cancer Res. 26 (1966) 1717–1721.
[26] M. Tada, Seryl-tRNA synthetase and activation of the carcinogen 4-nitroguinoline 1-oxide, Nature 255 (1975) 510–512.
[27] B. Bailleul, P. Daubersies, S. Galiegue-Zouitina, M.H. Loucheux-Lefebvre, Molecular basis of 4-nitroquinoline 1-oxide carcinogenesis, Jpn. J. Cancer Res. 80 (1989) 691–697.
[28] M. Nakajima, M. Kikuchi, K. Saeki, Y. Miyata, M. Terada, F. Kishida, et al., Mutagenicity of 4-nitroquinoline 1-oxide in the MutaMouse, Mutat. Res. 444 (1999) 321–336.
[29] R. Iannone, P. Campomenosi, C. Madzak, A. Inga, F. Caocci, A. Abbondandolo, Single stranded DNA-vectors for analyzing processing of DNA damage induced by 4-nitroquinoline-1-oxide in prokaryotes and eukaryotes, Boll. Soc. Ital. Biol. Sper. 68 (1992) 619–624.
[30] A. Inga, R. Iannone, P. Degan, P. Campomenosi, G. Fronza, A. Abbondandolo, P. Menichini, Analysis of 4-nitroquinoline-1-oxide induced mutations at the hprt locus in mammalian cells: possible involvement of preferential DNA repair, Mutagenesis 9 (1994) 67–72.
[31] Y. Shiraishi, A.A. Sandberg, Effects of various chemical agents on sister chromatid exchanges, chromosome aberrations, and DNA repair in normal and abnormal human lymphoid cell lines, J. Natl Cancer Inst. 62 (1979) 27–35.
[32] D. Wild, Cytogenetic effects in the mouse of 17 chemical mutagens and carcinogens evaluated by the micronucleus test, Mutat. Res. 56 (1978) 319–327.
[33] T. Nunoshiba, B. Demple, Potent intracellular oxidative stress exerted by the carcinogen 4-nitroquinoline-N-oxide, Cancer Res. 53 (1993) 3250–3252.
[34] H. Druckrey, R. Preussmann, S. Ivankovic, D. Schmahl, Organotropic carcinogenic effects of 65 various N-nitroso-compounds on BD rats, Z. Krebsforsch. 69 (1967) 103–201.
[35] N.E. Steidler, P.C. Reade, Experimental induction of oral squamous cell carcinomas in mice with 4-nitroquinolone-1-oxide, Oral Surg. Oral Med. Oral Pathol. 57 (1984) 524–531.

Effect of Running Training on DMH-Induced Aberrant Crypt Foci in Rat Colon

NORIYUKI FUKU[1], MASAKO OCHIAI[2], SHIN TERADA[1], ERI FUJIMOTO[1], HITOSHI NAKAGAMA[2], and IZUMI TABATA[1]

[1]*Division of Health Promotion and Exercise, National Institute of Health and Nutrition, Tokyo, JAPAN; and* [2]*Biochemistry Division, National Cancer Center Research Institute, Tokyo, JAPAN*

ABSTRACT

FUKU, N., M. OCHIAI, S. TERADA, E. FUJIMOTO, H. NAKAGAMA, and I. TABATA. Effect of Running Training on DMH-Induced Aberrant Crypt Foci in Rat Colon. *Med. Sci. Sports Exerc.*,Vol. 39, No. 1, pp. 70–74, 2007. **Purpose:** We examined the effects of treadmill-running training on the induction of aberrant crypt foci (ACF), which is the first step of colon cancer induction, in the colonic mucosa of rats injected with 1,2-dimethylhydrazine (DMH). **Methods:** Four-week-old F344 rats (N = 38) were randomly assigned to training (19 rats) and control (19 rats) groups. After a week, all rats were given DMH (20 mg·kg^{-1} body weight) once a week for 2 wk. Running training was started at age 7 wk (speed: 10 m·min^{-1}, 0% grade, 120 min·d^{-1}, 5 d·wk^{-1}). After 4 wk of training, the rats were sacrificed and the colon was removed, opened, and counted for ACF with 0.2% methylene blue staining. **Results:** Running training resulted in lower body- ($P < 0.01$) and adipose fat weight ($P < 0.05$). The numbers of ACF and total AC were significantly lower in the running training group than in the control group ($P < 0.05$). The occurrences of one, three, and five aberrant crypts per focus were also significantly lower in the running training group than in the control group ($P < 0.05$). The ratios of total AC/ACF did not significantly differ between the running training and control groups. **Conclusions:** The results of the present investigation suggest that low-intensity running training inhibits the DMH-induced initiation of colon ACF development. **Key Words:** EXERCISE, ACF, 1,2-DIMETHYLHYDRAZINE, COLON CANCER, PRIMARY PREVENTION, PHYSICAL ACTIVITY

Cancer of the large intestine is classified into colon and rectal cancers. The incidence of colon cancer is increasing at a faster rate than that of rectal cancer in recent years in advanced countries, including Japan. Colon cancers develop after the multistep accumulation of genetic and epigenetic induction of oncogenes in both humans and experimental animals (9,14,19).

The proposed multisteps of colon carcinogenesis may start when aberrant crypt foci (ACF) appear in the colon (37). ACF were defined as lesions composed of enlarged crypts, slightly elevated above the surrounding mucosa and more densely stained with methylene blue than normal crypts (3). ACF are considered to be putative preneoplastic colon lesions that may be early indicators of colon carcinogenesis (4,10,18).

Epidemiological evidence has suggested that physical activity has a protective effect on colon cancer incidence (11,13,30). However, few experimental studies have been conducted to elucidate the mechanisms of exercise-related effects on colon cancer. For example, a few earlier animal studies found that both voluntary (1,26) and treadmill (36) running training reduced tumor incidence after the administration of 1,2-dimethylhydrazine (DMH) or azoxymethane. Furthermore, no studies have examined the effects of physical exercise training on colon cancer as they might be related to the multistep nature of colon carcinogenesis, although Demarzo et al. (7) recently reported that a single session of exhaustive exercise increased the number of ACF DMH-induced rat colons. Up to now, there is no study demonstrating that exercise training affects the number of ACF, which is a putative initial step of colon carcinogenesis of rats. Therefore, we investigated the effects of running exercise training on the number of DMH-induced ACF, because previous studies suggested that physical training of this type has a protective effect on colon tumor incidence in rats.

Address for correspondence: Izumi Tabata, Ph.D., FACSM, Division of Health Promotion and Exercise, Incorporated Administrative Agency National Institute of Health and Nutrition, 1-23-1 Toyama, Shinjuku City, Tokyo, 162-8636, Japan; E-mail: tabata@nih.go.jp.
Submitted for publication March 2006.
Accepted for publication July 2006.

0195-9131/07/3901-0070/0
MEDICINE & SCIENCE IN SPORTS & EXERCISE®

DOI: 10.1249/01.mss.0000239398.78331.96

MATERIALS AND METHODS

Materials

All chemicals, including 1,2-dimethylhydrazine (DMH), a carcinogenic chemical of the colon, was purchased from SIGMA (St. Louis, MO).

Exercise Protocols

Animal care. All experimentation was conducted in accordance with policy statement of the American College of Sports Medicine on research with experimental animals and was approved by the animal care and use committee of National Institute of Health and Nutrition. Four-week-old Fischer 344 male rats were purchased from CLEA Japan, Tokyo. The animals were housed in rooms lighted from 7 a.m. to 7 p.m. and were maintained on an *ad libitum* diet of standard chow and water. The room temperature was maintained at 20–22°C.

Experimental design. After 1 wk of acclimatization to the housing environment (5 wk of age), the rats were randomly assigned to one of two groups: the treadmill-running training group (N = 19) or the control group (N = 19). All rats were given a subcutaneous injection of DMH at a dose level of 20 $mg \cdot kg^{-1}$ body weight, once a week for 2 wk. The DMH was dissolved in 0.1 mM EDTA (pH 6.5) immediately before the administration.

One week after the last injection of DMH (i.e., at age 7 wk), running training was started. The training rats ran for 120 $min \cdot d^{-1}$ (two 60-min bouts separated by 10 min of rest) on a flat motorized treadmill (Natsume, Tokyo, Japan). On the first day, the rats were accustomed to running at a speed of 10 $m \cdot min^{-1}$ by gradually increasing the treadmill speed to the fixed speed. The running speed was maintained for the following 4 wk of training. The intensity of this training was considered to be low because this exercise could be continued for more than 6 h without exhaustion, as reported elsewhere (34).

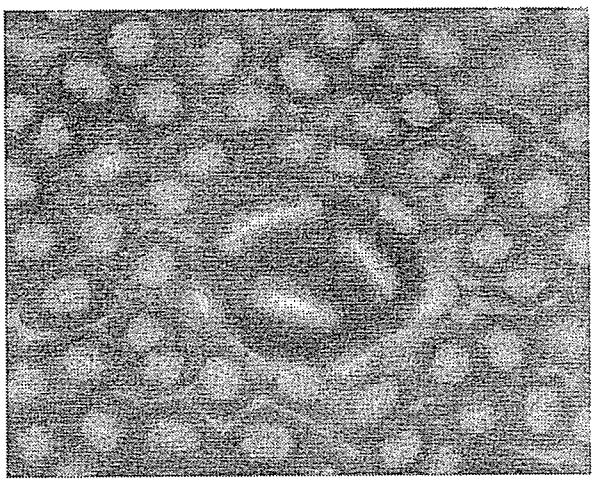

FIGURE 1—1,2-dimethylhydrazine–induced ACF in methylene blue–stained colonic mucosa. In particular, ACF is indicated by the three aberrant crypts per focus that have large crypts, altered luminal openings, and thickened epithelia. This micrograph shows an ACF that consists of three AC. ACF, aberrant crypt foci; AC, aberrant crypts.

TABLE 1. The effect of treadmill-running training on body weight, muscle weight of the heart and soleus, adipose tissue weight of the peritoneum and epididymides, and citrate synthase activity of soleus muscle in rats.

	Control Group (N)	Training Group (N)
BW (g)	216.7 ± 3.5 (19)	199.1 ± 4.0 (19)$^{\#\#}$
Heart weight ($mg \cdot g^{-1}$ BW)	2.89 ± 0.04 (11)	3.00 ± 0.04 (10)$^{\#}$
Soleus weight ($mg \cdot g^{-1}$ BW)	0.33 ± 0.01 (19)	0.37 ± 0.01 (19)$^{\#\#}$
Peritoneal adipose tissue weight ($mg \cdot g^{-1}$ BW)	15.0 ± 0.7 (19)	10.2 ± 0.6 (19)$^{\#\#\#}$
Epididymides adipose tissue weight ($mg \cdot g^{-1}$ BW)	15.1 ± 0.7 (19)	10.2 ± 0.6 (19)$^{\#}$
Brown adipose tissue weight ($mg \cdot g^{-1}$ BW)	1.50 ± 0.07 (11)	1.28 ± 0.10 (10)
Citrate synthase activity in soleus muscle ($\mu mol \cdot g^{-1}$ wet tissue$\cdot min^{-1}$)	35.9 ± 1.0 (19)	40.3 ± 1.2 (19)$^{\#\#}$

Values are means ± SE. BW, body weight. $^{\#}$, $^{\#\#}$, $^{\#\#\#}$ indicate significant differences from the control group at levels of $P < 0.05$, 0.01, and 0.001, respectively, by t-test.

Two or three days after the last bout of exercise, the rats were anesthetized with an intraperitoneal injection of pentobarbital sodium (50 $mg \cdot kg^{-1}$ body weight), and the heart and soleus muscles were excised, weighed, quickly clamp-frozen in liquid nitrogen, and stored at −80°C until analysis. Then, the colons were dissected and gently flushed with 10% neutralized formalin to remove residual bowel contents, cut open longitudinally, fixed flat between filter papers, and submerged in 10% neutralized formalin overnight at 4°C (23). Peritoneal fat, epididymides fat, and brown adipose tissue (BAT) were excised and weighed.

Detection of ACF. Fixed colons were stained with 0.2% methylene blue, as described by Bird (3). The number of ACF and total number of aberrant crypts (AC) comprising ACF were counted for each colon. The ratio of total AC/ACF was calculated to assess ACF multiplicity. As shown in Figure 1, ACF were identified as lesions composed of enlarged crypts, with an increased pericryptal area, a slightly elevated appearance above the surrounding mucosa with an oval or slitlike orifice, and a higher staining intensity with 0.2% methylene blue than normal crypts (3).

Citrate synthase activity in skeletal muscle. Ten percent homogenates were made from the muscle in 175 mM KCl, 10 mM glutathione, and 2 mM EDTA, pH 7.4. The homogenate was frozen and thawed four times and mixed thoroughly before enzymatic measurements. As a maker of oxidative enzyme, citrate synthase (CS) activity in the soleus muscle was measured using Srere's method (31).

Statistical Analysis

All data are shown as the mean ± SE. Quantitative clinical data were compared between run-trained rats and controls by use of the unpaired t-test. ACF-related data were also compared by use of the Mann–Whitney rank sum test because the numbers of ACF were not normally distributed. These data were analyzed by use of SigmaStat for Windows (SPSS Inc., Chicago, IL). Differences were considered significant when the P value was less than 0.05.

RESULTS

Physical characteristics and citrate synthase activity. The body weight of the training rats was